

1 The authors would like to thank the two anonymous reviewers for their helpful comments and
2 suggestions. All comments are addressed below. Comments are included in italics and author
3 responses are in plain text. The revised manuscript (with changes shown) has been included at
4 the end this document.

5 **Note that sections “Gas-Particle Partitioning of Organic Nitrates” and “Hydrolysis of**
6 **Organic Nitrates” were switched to improve the manuscript readability. Figure numbers**
7 **have changed and these changes are pointed to in this response document. Changes to**
8 **figure numbers are as follows:**

9 **Fig. 3 → Fig. 4**

10 **Fig. 4 → Fig. 5**

11 **Fig. 5 → Fig. 3**

12

13 **Reviewer #1**

14 *1 – The statement about observed hydrolysis rate in the abstract does not match your discussion and last*
15 *figure, which suggests a dependence of hydrolysis on RH. I think this rate should be reported cautiously*
16 *and I would avoid stating a cutoff for hydrolysis given the lack of reproducibility in your measurements*
17 *near 22%.*

18 We have clarified and expanded the discussion of the non-linear dependence of hydrolysis on RH in the
19 abstract of the revised manuscript. The relevant excerpt now reads:

20 “Particle-phase ON hydrolysis rates consistent with observed ON decay exhibited a nonlinear
21 dependence on relative humidity (RH): An ON decay rate of 2 day^{-1} was observed when the RH ranged
22 between 20 and 60%, and no significant ON decay was observed at RH lower than 20%. In experiments
23 when the highest observed RH exceeded the deliquescence RH of the ammonium sulfate seed aerosol,
24 the particle-phase ON decay rate was as high as 7 day^{-1} and more variable.”

25 We note that we are not the first to report an abrupt increase in nitrate loss rate with increasing RH. Liu
26 et al. (2012) reported a loss rate of 0 up to ~18% RH but saw a consistent loss rate of 4 day^{-1} at 40% RH
27 and above.

28 *2 – P. 20635, re: wall loss correction: How would this correction be affected if wall loss rates depend on*
29 *RH (likely) or are different for different chemical species?*

30 As part of the applied wall loss correction the organic PM in each experiment was normalized to the
31 ammonium sulfate from the same experiment. This correction assumes that the concentrations of
32 ammonium sulfate PM only change due to wall loss and that the wall loss rates of organic PM is equal to

33 the wall loss rate of ammonium sulfate (i.e. that the organics and ammonium sulfate form an internal
34 mixture). A main advantage of this correction method is that variation of wall losses between
35 experiments is accounted for; therefore differences in wall losses with RH are accounted for using this
36 correction.

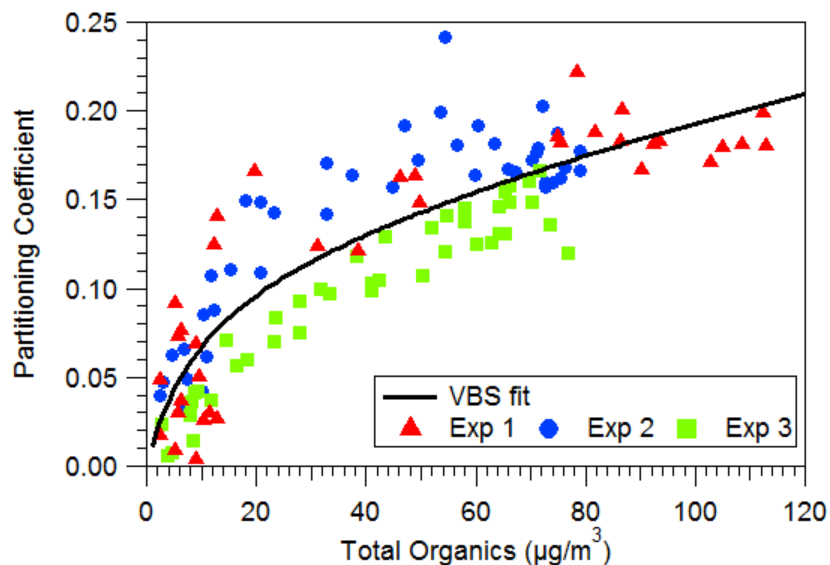
37 *3 – P. 20636, obtaining mixing ratio of aerosol nitrate: Please flesh out explanation of this. Did you take*
38 *mass loading of each NO and NO₂ separately and use those fragments' MW's to convert to mixing*
39 *ratios, which you then summed? Doesn't the AMS calibration assume that both NO and NO₂ come from*
40 *NO₃ functional groups and therefore the MW to use to do the conversion would be that of the NO₂*
41 *fragment, since it is assumed the O-N bond breaks and one of the O's would be detected among the*
42 *organic fragments? Please clarify what you did and be sure that the assumptions are correction – this*
43 *could give big errors in the mixing ratios and consequently change the partitioning coefficients*
44 *substantially!*

45 This has been corrected. The reviewer is correct that each NO₊ and NO₂⁺ fragment measured in the
46 ACSM originates from an NO₃ functional group so the MW of 62 g/mol should be used to convert mass
47 concentrations to mixing ratios. The resulting changes to partitioning coefficient are now discussed in
48 further detail in the manuscript:

49 “the mass concentration of nitrate measured by the ACSM was converted to mixing ratio (ppb) using the
50 molecular weight of the nitrate functional group (62 g/mol)”

51 An updated Figure 5 (partitioning coefficient, previously Fig. 4) and discussion of the results has been
52 included below. The Rollins et al. VBS fit has been removed from Fig. 5 as it was only relevant below 10
53 μg/m³ (the concentrations measured in the 2010 CalNex field campaign).

54 “As seen in Fig. 5 these results indicate that under typical ambient conditions (< 40 μg/m³ of OA) 5-10%
55 of organic nitrates formed from the photo-oxidation of α-pinene under high NO_x conditions are
56 expected to partition to the particle phase. This is significantly lower than the organic nitrate
57 partitioning calculated by Rollins et al. (2013) for organic nitrates measured in Bakersfield, CA during the
58 CalNex campaign in 2010. In those measurements >30% partitioning of ON was observed at organic
59 aerosol concentrations of 10 μg/m³. The difference could be attributed to differences in precursor
60 molecules and levels of oxidation. Studies have shown that high NO_x conditions can shift photochemical
61 oxidation products of terpenes towards higher volatility compounds (Wildt et al. 2014). Rollins et al.
62 determined using the SPARC model (Hilal et al., 2003) that precursor molecules (a mix of C₅-C₁₅ VOCs)
63 would need two stages of oxidative chemistry beyond the initial oxidation of the VOC to reach the point
64 when 19-28% would partition to the particle phase for a C_{OA} of 3 μg m⁻³. This may suggest that the ON
65 formed in our experiments have undergone fewer than three generations of oxidation as they are more
66 volatile than the ON measured in Bakersfield during CalNex 2010.”



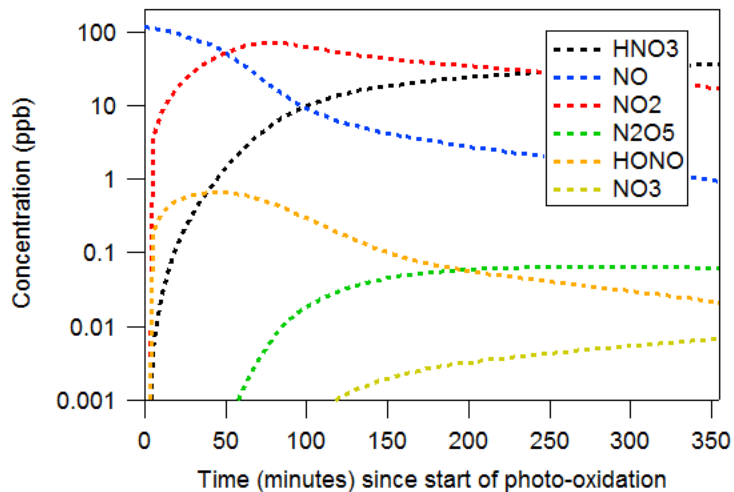
67

68 Figure 5 – Volatility basis set fit from this work shown with data from Expts. 1, 2, and 3.

69 *4 – Ibid. I have serious reservations about the accuracy of the determination of gas-phase organonitrates*
 70 *from mass balance. This assumes there are no other N-containing species, such as HONO or NO₃ and*
 71 *N₂O₅, which could certainly form in your experiments. Photolysis of these may be fast, but so might the*
 72 *production rate. You could include these in your model to show their expected concentrations and then*
 73 *determine whether they could be a source of error to your N balance. At least in the supplemental*
 74 *material, please show one of your time series of the partitioning coefficient.*

75 Figure S2 has been added which shows a time series of all N containing compounds formed in these
 76 experiments according to the SAPRC model. The time series shows that concentrations of HONO, NO₃
 77 and N₂O₅ are orders of magnitude lower than the 5 compounds included in the mass balance. The error
 78 associated with ignoring HONO, NO₃ and N₂O₅ in the mass balance is therefore low and within the
 79 uncertainty of our experiments. A brief discussion of this has been added to the manuscript:

80 “Figure S2 shows that, based on the Statewide Air Pollution Research Center (SAPRC) model
 81 (<http://www.engr.ucr.edu/~carter/SAPRC/>), the concentrations of other forms of reactive nitrogen are
 82 orders of magnitude lower than the concentrations of these five forms.”



83

84

Figure S2 – SAPRC results from Expt. 7 showing significant nitrogen compounds

85 *5 – P. 20637, discussion of hydrolysis rate: From Darer et al, it appears that tertiary nitrates should have*
 86 *rapid hydrolysis rate constants and primary should be quite slow. Boyd et al ACPD 2015 have used this to*
 87 *estimate in the case of NO₃ + β-pinene, what fraction of the NO₃ radical additions occur at which end of*
 88 *the double bond. This might be worth discussing here. Do you assume that all of your nitrate is tertiary*
 89 *and compare to the literature based on that? Is there any literature basis for a faster rate than the one*
 90 *you assume in your assessment of whether the gas/aerosol partitioning could be affected by hydrolysis?*
 91 *My sense was that these rates are not well known. You conclude hydrolysis can't affect partitioning – is*
 92 *this because the assumed hydrolysis rate was slow relative to the timescale of these experiments? Given*
 93 *the uncertainties in hydrolysis rates, you could flip this analysis around and ask instead, how fast does*
 94 *the hydrolysis have to be to change the partitioning coefficient by X%? Perhaps in addition to what you*
 95 *have here. This would give future researchers a quick comparison point – if they determine a faster rate,*
 96 *this provides a quick assessment of whether that rate is partitioning-relevant.*

97 The difference between 10% of ON hydrolysis observed by Boyd et al. 2015 and this study is an
 98 important one as it shows the potential differences between ON formed from NO₃ (Boyd) and ON
 99 formed from OH + NO (this study). There are also differences in how β-pinene and α-pinene are
 100 oxidized. More discussion of this has been added to the revised manuscript. :

101 “Boyd et al. (2015) measured a lifetime of 3-4.5 hours for 10% of ON formed from NO₃ oxidation of β-
 102 pinene, with a much longer lifetime for the remaining 90%. This suggests that 10% of the ON functional
 103 groups were tertiary with the rest being primary or secondary as those have been shown to hydrolyze
 104 much slower in the bulk phase (Darer et al., 2011; Hu et al., 2011). In our results hydrolysis is not limited
 105 to 10% of ON, suggesting that a higher portion is tertiary ON functional groups.”

106 “Similar VOC precursors such as α-pinene and β-pinene can form different fractions of
 107 primary/secondary and tertiary ON. When NO₃ reacts and bonds with the terminal double bond of β-
 108 pinene, an alkyl radical is formed in either a primary or tertiary position (opposite of the carbon-nitrate
 109 bond). The tertiary alkyl radical is more stable, so primary organic nitrates are expected to be more

110 abundant. The double bond in α -pinene is not terminal, so the NO_3 reaction produces either a secondary
111 or tertiary ON and alkyl radical. NO_3 typically bonds with the less substituted carbon of a double bond so
112 that a more highly substituted alkyl radical is formed. The reverse is true for OH+NO chemistry. In this
113 case NO reacts with the peroxy-radical to form the nitrate group. The peroxy-radical, a product of O_2
114 and an alkyl radical, is likely to be on a more substituted carbon as this would have been the more stable
115 alkyl radical. Thus, more highly substituted ON are expected from OH + NO_x than from NO_3 chemistry.
116 This has important implications for attempts to model ON and the resulting NO_x recycling.”

117 On the topic of hydrolysis affecting partitioning: The 12 hour lifetime we measured for ON in PM at mid-
118 level RH was used to find the maximum deviation in partition coefficient in Expt. 2. This was the only
119 experiment used to calculate partitioning which had high enough RH to be significantly affected by
120 hydrolysis. When the partition coefficient in this experiment was 0.2, the maximum seen in the data
121 used in calculation of the VBS, if hydrolysis had not occurred the partition coefficient would increase
122 from 0.2 to 0.23. This is the maximum effect that hydrolysis could have on the partitioning coefficient,
123 with lower effects earlier in the experiment and no significant effects on the low RH experiments.

124 *6 – P. 20639, interpreting the <0 values: You mention the possibility of HNO_3 contributing to aerosol*
125 *nitrate. A calculation using Henry’s law coefficient for HNO_3 will allow you to determine whether this*
126 *could be happening.*

127 The negative values were not anymore present after correcting the calculation of particulate nitrate as
128 detailed in the response to comment 3. However a Henry’s Law calculation shows that total particulate
129 HNO_3 is 3 orders of magnitude lower than the total amount of HNO_3 in the gas phase under the
130 conditions of these experiments. This detail has been added to the revised manuscript:

131 “All PM nitrate (measured by the ACSM as NO^+ and NO_2^+ fragments) was assumed to be organic because
132 no inorganic nitrate was introduced in these controlled experiments. Nitric acid is formed in the gas
133 phase as well as in the particle phase through hydrolysis, but it is assumed that nitric acid
134 concentrations are negligible in the particle phase due to its high vapor pressure (Fry et al., 2009). A
135 Henry’s Law calculation suggests that the total amount of aqueous HNO_3 in particles is 3 orders of
136 magnitude lower than that in the gas phase.”

137 *7 – P. 20640, interpreting temperature ramps: Were these only done during the early states of oxidation,*
138 *while the partitioning species would be the less oxidized and thus more semi-volatile? Or did you try this*
139 *at different delay times to investigate the effect of increasing oxidation on (presumably) decreasing*
140 *volatility?*

141 These temperature changes were conducted at the end of the experiment, primarily to confirm that
142 organic nitrate species are semi-volatile.

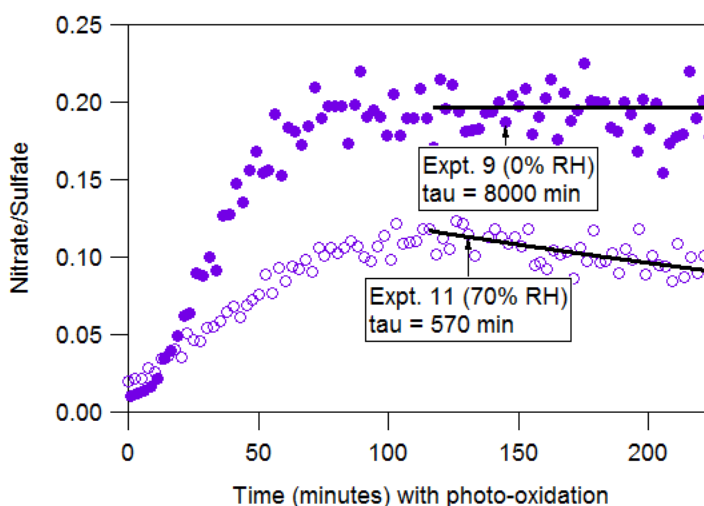
143 *8 – P. 20642 bottom, discussion of observation of decrease in both organics and nitrate: why should PM*
144 *organics also decrease? Hydrolysis producing HNO_3 would certainly be expected to volatilize the nitrate,*
145 *but mightn’t the organic left behind be expected to stay in the condensed phase? Can you learn anything*
146 *from the relative rates of loss of organic vs NO_3 ?*

147 PM organics did not decrease as significantly or consistently as PM nitrate and the discussion in the
148 manuscript has been modified to more accurately describe this:

149 “Concentrations of wall-loss corrected PM nitrate (normalized to SO_4) were observed to decrease
150 towards the end of most experiments ... PM organics also decreased in some experiments, but their
151 loss rate was lower and more variable than that of nitrate. Based on the work by Chuang et al. (2015)
152 the addition of a nitrate functional group decreases volatility of a compound by 2.5 orders of magnitude
153 – slightly more than the resulting alcohol group from hydrolysis. Thus, the organic compound resulting
154 from ON is more volatile than the original organic nitrate, and as a result could partition to the gas
155 phase, resulting in a decrease in PM organics.”

156 *9 – Ibid, + around p. 20643 line 1-3: please explain how you obtained these hydrolysis rates- just the*
157 *decay rate of NO_3 aerosol? Or normalized to SO_4 ?*

158 An exponential was fit to NO_3 normalized to SO_4 . This has been clarified in the manuscript and in
159 addition a new figure (S4) has been added to the SI to illustrate calculation of the hydrolysis rate:



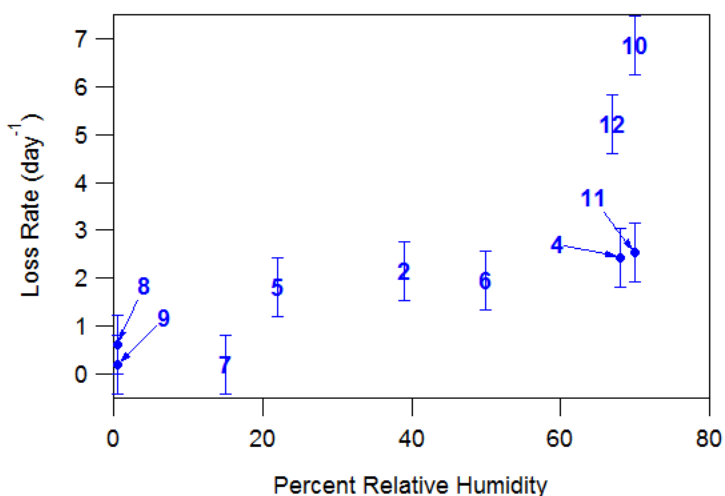
160
161 Figure S4 – Exponential decay for a low RH (Expt. 9) and high RH (Expt. 11) conditions

162 *10 – Table 1: Looking at the hydrolysis rates here for RH = 22, 15, and the two 70’s, I am not convinced of*
163 *the reproducibility at a given RH. This either just means the rates are not known that well, or that RH is*
164 *not the determining factor. Either way, I think this suggests a retreat from Fig. 5, which implies that*
165 *there is a correlation between RH and NO_3 loss rate.*

166 An additional experiment was conducted at high (67%) RH and the results warranted additional
167 discussion and an update to Fig. 3 (previously Fig 5):

168 “Experiments conducted at an average RH of 67% or higher can exhibit a significantly higher decay rate,
169 probably due to effects of being near the deliquescence relative humidity of the ammonium sulfate seed
170 aerosol. In experiments 10 and 12, which have decay rates well above 2 day^{-1} , the chamber was initially
171 cooled to 20°C before the UV lights were turned on. Once the UV lights were activated the temperature

172 then increased to 25 °C and the RH settled at the values indicated in Table 1. For these experiments the
 173 RH was above 80% (the deliquescence RH, DRH, of $(\text{NH}_4)_2\text{SO}_4$ for several minutes, potentially resulting in
 174 aqueous aerosol. Experiment 11 also reached a relative humidity above deliquescence, yet it shows a
 175 lower nitrate loss rate than Expts. 10 and 12. The ratio of organics and nitrates to sulfate (seed) particles
 176 was much lower in Expt. 11 compared to Expts. 10 and 12, but whether and why this would result in a
 177 different nitrate loss rate is currently unclear. The relative humidity in Expt. 4 did not reach the DRH of
 178 $(\text{NH}_4)_2\text{SO}_4$. Future work should focus on the fate of ON at higher (> 60%) relative humidity. The generally
 179 higher nitrate loss rate at higher RH makes hydrolysis of particulate nitrate functional groups the most
 180 plausible explanation for the observed decay.”



181

182 Figure 3. The organic nitrate loss rate as a function of relative humidity.

182

183 *11 – Figure 2 is puzzling to me. Why don't the intermittent green traces match their previous trend? You*
 184 *interpret this as meaning that the more oxidized species are monotonically increasing, but that is not*
 185 *apparent here; they appear to have decreased around 200 minutes. This requires more*
 186 *explanation/interpretation.*

187 We have since learned that there are start-up effects when the reagent ion is switched in the CIMS. The
 188 sensitivity slowly adjusts to a steady state value over the first ~20 minutes after start-up. Despite these
 189 issues with short-term trends the long-term trends are still useful. This has been clarified in the revised
 190 manuscript:

191 “In short time periods after switching reagent ions the sensitivity of the HR-ToF-CIMS slowly adjusts to a
 192 steady state value. Minor changes during these short time periods should be taken with caution but the
 193 overall trends over the 4.5 hour experiment are useful in viewing oxidation trends.”

194 *12 – Figure 3: the re-increase of the particle phase signals after cooling that you mention in the text isn't*
 195 *super clear to me here – clearer is the gas phase loss. Maybe this suggests that the re-condensing species*
 196 *are mostly partitioning to the walls? Could discuss in terms of relative SA of particles vs. walls.*

197 It is true that in this cooling phase many compounds are likely lost to the walls as these are the coolest
198 location of the chamber during active cooling. The primary purpose of this figure is to show that organic
199 nitrates are semi-volatile, as shown by their evaporation upon heating. The temperature data is not
200 used in a quantitative way in calculating partitioning. More discussion has been added to the revised
201 manuscript:

202 “Other processes may influence particle and gas concentrations of organic compounds. Continuing
203 reactions with O₃ and nitrate radicals (since O₃ and NO₂ are both present) limit the ability to stop all
204 chemical activity. This is seen in the gas phase compounds, some of which appear to be changing in
205 concentration after the UV lights are off. Despite this a clear change is seen in all compounds with a
206 temperature increase. During the cooling phase (beginning at t = 320 minutes) the particle phase
207 organic and nitrate concentrations do not return to the original levels. It is likely that some organic
208 compounds are lost to the walls of the Teflon chamber, especially since they reach the coldest
209 temperatures during active cooling, and thus Org/SO₄ does not return to the values seen before
210 temperature changes began. Despite these limitations it is clear that both the Org/SO₄ and ON^{aer}/SO₄
211 ratios decrease with heating, consistent with semi-volatile organics and organic nitrates.”

212 *13 – Figure 4 comparison: Is the Rollins et al VBS fit also based on mole fraction, not mass fraction?*
213 *Could this matter here for the discrepancy?*

214 Rollins et al also uses a mole basis as their measurements are done with thermal dissociation-laser
215 induced fluorescence (TD-LIF), which converts all organic nitrates to NO₂ before detection. Thus, this is
216 not expected to be related to the observed difference. There is a different way that the measurement
217 method may contribute to differences, which has been noted in the revised manuscript:

218 “It should also be noted that the thermal dissociation-laser induced fluorescence (TD-LIF) instrument
219 used by Rollins et al. (2013) has been shown in a recent study to measure PM ON a factor of two higher
220 than the ON measured by aerosol mass spectrometers (Ayres et al., 2015) which utilize similar
221 measurement and detection techniques as the ACSM used in this work. While the reasons for this
222 difference are unknown it would result in a higher partitioning coefficient compared to the one
223 calculated from the AMS (or ACSM) and explain part of the observed difference.”

224 *14 – Suggest to omit Figure 5. I’m not convinced RH is the driving factor here.*

225 While RH may not be the only factor affecting the observed nitrate loss rate, our data do suggest that
226 the RH affects hydrolysis in a non-linear way, as further discussed in our response to comments 1 and
227 10. Previous work (Liu et al., 2012; Boyd et al., 2015) has also found that ON hydrolysis proceeds under
228 humid conditions but not under low RH. Other measured factors such as precursor concentration, OH
229 levels and organic aerosol levels were analyzed for correlation with nitrate loss rate and no consistent
230 trend was found.

231 *15 – Supplemental Fig. S2: O3 goes up quite a bit over your experiments – could this compete with OH for*
232 *your α-pinene? Or react with NO2 and affect N balance (this is where I started wondering about whether*
233 *N2O5 could be another part of the N balance story). Is NO2+O3 in your SAPRC model?*

234 The two major pathways of ON formation are OH+NO or direct oxidation by NO₃. Ozone and NO₂ can
235 react to form NO₃ but this is quickly photolyzed and does not compete in ON formation in these
236 experiments. Ozone formation in these experiments is roughly proportional to OH concentrations, and
237 thus H₂O₂ concentrations. Thus, experimental conditions had similar ratios of these oxidants. The
238 lifetime of α-pinene is similar at the OH or O₃ levels in these experiments. Regardless, the interest of
239 these experiments is the organic nitrates formed in the oxidation of α-pinene through NO reacting with
240 the peroxy-radical. Some of the ozone is expected to react with α-pinene, but the ozonolysis of α-pinene
241 is not expected to result directly in ON, which is the focus of this work.

242

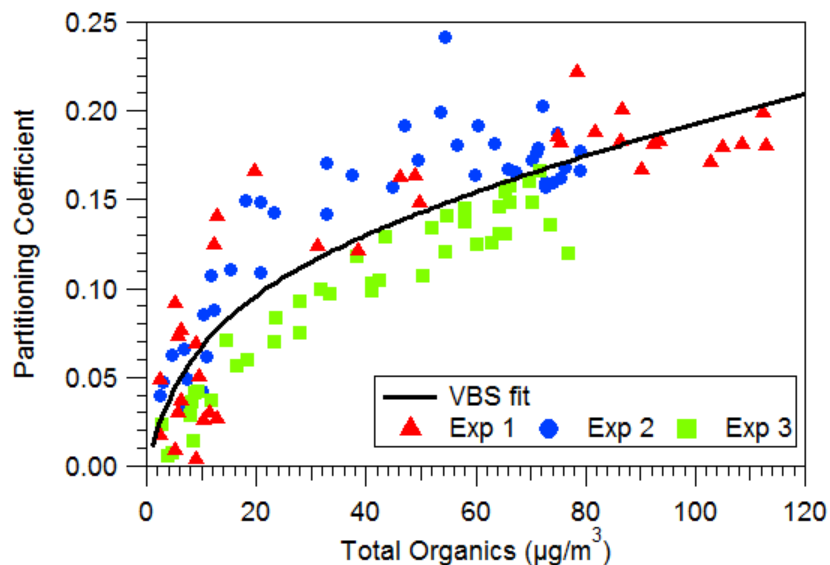
243 **Responses to Reviewer #2**

244 *1 – Page 20636, line 21. The authors noted that the NO and NO₂ fragments were converted to ppb using*
245 *the molecular weight of these fragments. I do not think this is correct. The NO and NO₂ mass*
246 *concentrations are nitrate (-ONO₂) equivalent mass, so to convert them into molar basis, the molecular*
247 *weight of -ONO₂ should be used. If the authors indeed calculated the mixing ratios incorrectly, it would*
248 *change the partitioning coefficients and affect the conclusions of the manuscript.*

249 The manuscript has been corrected and Figure 5 (previously Fig. 4) has been adjusted. Additional
250 discussion has been added about the partitioning and differences between this and the previous work
251 by Rollins et al. 2013. The VBS fit for Rollins et al. 2013 has been removed as their data were mainly
252 relevant below 10 µg/m³) The manuscript has been updated (as previously discussed in response to
253 Reviewer 1, #3):

254 “the mass concentration of nitrate measured by the ACSM was converted to mixing ratio (ppb) using the
255 molecular weight of the nitrate functional group (62 g/mol)”

256 “As seen in Fig. 5 these results indicate that under typical ambient conditions (< 40 µg/m³ of OA) 5-10%
257 of organic nitrates formed from the photo-oxidation of α-pinene under high NO_x conditions are
258 expected to partition to the particle phase. This is significantly lower than the organic nitrate
259 partitioning calculated by Rollins et al. (2013) for organic nitrates measured in Bakersfield, CA during the
260 CalNex campaign in 2010. In those measurements >30% partitioning of ON was observed at organic
261 aerosol concentrations of 10 µg/m³. The difference could be attributed to differences in precursor
262 molecules and levels of oxidation. Studies have shown that high NO_x conditions can shift photochemical
263 oxidation products of terpenes towards higher volatility compounds (Wildt et al. 2014). Rollins et al.
264 determined using the SPARC model (Hilal et al., 2003) that precursor molecules (a mix of C₅-C₁₅ VOCs)
265 would need two stages of oxidative chemistry beyond the initial oxidation of the VOC to reach the point
266 when 19-28% would partition to the particle phase for a C_{OA} of 3 µg m⁻³. This may suggest that the ON
267 formed in our experiments have undergone fewer than three generations of oxidation as they are more
268 volatile than the ON measured in Bakersfield during CalNex 2010.”



269

270 Figure 5 – Volatility basis set fit from this work shown with data from Expts. 1, 2, and 3.

271 2 – Page 20637, section 2.2. The calculation of partitioning coefficient is subjected to many
 272 uncertainties, which should be discussed in detail and the authors should evaluate how such
 273 uncertainties might affect the conclusions of the manuscript.

274 a. It is assumed that only five major forms of oxidized nitrogen are present. As this assumption forms the
 275 basis of the subsequent analysis, the authors need to justify this assumption. Other nitrogen-containing
 276 species can be formed in their experiments, e.g., NO₃, N₂O₅, HO₂NO₂ (especially H₂O₂ is used as OH
 277 precursor, which would lead to formation of a large amount of HO₂), HONO, etc. These species could be
 278 photolyzed or react with OH, but the authors need to provide justifications that all other nitrogen-
 279 containing species are negligible. If not, how would this affect the calculation of partitioning coefficient?

280 Please reference the response to Reviewer 1, comment #4. Other species which contain reactive
 281 nitrogen have been added to a new figure (S2) which shows that concentrations are several orders of
 282 magnitude lower than the five major forms.

283 b. It is noted that the H₂O₂ concentration used in the model was adjusted until the modeled NO, NO₂,
 284 and O₃ matched experimental data. Firstly, why is the H₂O₂ concentration not an input? Based on the
 285 experimental description, the concentration of H₂O₂ should be known (e.g., can be calculated from the
 286 injected H₂O₂ volume and chamber volume). Secondly, as seen in Table 1, the modeled H₂O₂ has a large
 287 variation. Is this expected? i.e., did the authors inject different amounts of H₂O₂ into the chamber in
 288 different experiments? If so, what are the H₂O₂ concentrations injected (this info needs to be include
 289 in the table)?

290 In experiments 1, 2, and 3 (the experiments which were used to calculate partitioning) the H₂O₂ was
 291 injected by passing air through a solution of H₂O₂ and then into the chamber. Thus, the amount injected
 292 was not known and this had to be estimated by tuning the concentrations of NO, NO₂, and ozone in the
 293 SAPRC model. In the other experiments a measured liquid volume of H₂O₂ was heated as air was passed

294 over it and into the chamber. The volume of H₂O₂ injected was varied between experiments but did not
295 match the model results - the model matched data for NO, NO₂ and ozone at H₂O₂ levels lower than
296 those injected. This could be because the injection method was not efficient, or it could be that the
297 photolysis of H₂O₂ (which ultimately drives the concentrations of NO, NO₂ and ozone) is not accurately
298 represented in the model. The absorption cross section of H₂O₂ only minimally intersects with the UV
299 spectrum. Thus, small changes in the UV spectrum (or errors in measurements of the spectrum) could
300 cause significant errors in estimated concentrations of [OH].

301 *c. If the H₂O₂ concentration indeed varies that much, it would seem very likely that the fraction of α-*
302 *pinene reacting with OH vs. O₃ also varies from experiment to experiment. Would different types of*
303 *organic nitrates be formed in different experiments, depending on the reaction pathways? If so, how*
304 *would this contribute to the calculation of the partitioning coefficient of organic nitrates as a whole?*

305 As discussed in response to Reviewer 1, #15: The two major pathways of ON formation are OH+NO or
306 direct oxidation by NO₃. Ozone and NO₂ can react to form NO₃ but this is quickly photolyzed and does
307 not compete in ON formation in these experiments. Ozone formation in these experiments is roughly
308 proportional to OH concentrations, and thus H₂O₂ concentrations. So experimental conditions had
309 similar ratios of these oxidants. The lifetime of α-pinene is similar at the OH or O₃ levels in these
310 experiments. Regardless, the interest of these experiments is the organic nitrates formed in the
311 oxidation of α-pinene through NO reacting with the peroxy-radical. Some of the ozone is expected to
312 react with α-pinene, but the ozonolysis of α-pinene is not expected to result directly in ON, which is the
313 focus of this work.

314 *d. Related to the previous comment – from Figure S2 it appears that the ozone concentration is quite*
315 *high. Is the α-pinene concentration measured? If so, it should be included in Figure S2.*

316 Measurements of α-pinene were not possible in these experiments because other peaks interfere with
317 its measurement with the HR-ToF-CIMS; however, according to the model all the α-pinene has reacted
318 well before the exponential is fit to the ON loss rate in the particle phase. As mentioned in the response
319 to the comment above the lifetimes of α-pinene towards reaction with OH and O₃ were similar based on
320 the end of experiment concentrations, but the slow build-up of ozone in the first hour means that the
321 majority of α-pinene reacts first with ·OH.

322 *e. This comment is not just relevant for the determination of the partitioning coefficient, but also*
323 *relevant for the evaluation of organic nitrate hydrolysis. ACSM is a unit mass resolution instrument and*
324 *cannot differentiate ions at the same mass. E.g., m/z 30 can be CH₂O⁺ and NO⁺. Here, I guess the*
325 *authors assume that all m/z 30 is from NO⁺. How did the authors justify this assumption? It has been*
326 *shown that for organic nitrates formed from β-pinene+NO₃ (Boyd et al., 2015), the organic CH₂O⁺*
327 *fragment accounts for a fairly fraction of the total signal at m/z 30. If this applies for the current study,*
328 *the particle-phase organic nitrate would be over-estimated, which would affect the calculated partition*
329 *coefficient. It is possible that the organic interference at m/z 30 would depend on the particular system.*
330 *However, the authors need to discuss what does this mean for their data analysis and conclusion.*

331 The standard fragmentation table is used to calculate NO⁺ (Allan et al., 2004). Based on this table a
332 portion of the m/z 30 signal is allocated to (N₁₅)₂⁺ based on the measured N₂⁺. A portion is also allocated
333 to organics, as the reviewer suggests; and the remainder is attributed to NO⁺. There is of course
334 uncertainty associated with using the standard fragmentation table. We are currently planning future
335 experiments in which we will measure organic nitrates using a high resolution time of flight aerosol mass
336 spectrometer (HR-ToF-AMS). With data from the HR-ToF-AMS we will be able to evaluate the validity of
337 this standard fragmentation table by comparing unit mass with high resolution data; in the meantime
338 we are using the standard approach to separate nitrate mass used in unit mass resolution analysis. We
339 do not own a HR-ToF-AMS (the planned experiments are with a borrowed instrument) and therefore do
340 not have the high resolution data available for these experiments.

341 *3. Page 20639. Figure 2. Are these the only organic nitrate species measured in the experiments? Please*
342 *clearly state this in the manuscript.*

343 The compounds shown in Figure 2 are a selected few of many which are observed with the CIMS. This
344 has been clarified in the revised manuscript:

345 “Many compounds are identified with the CIMS and a select few of the most prominent compounds
346 were chosen for Fig. 2”

347 *4. Page 20640, discussion on gas-particle partitioning. The authors changed the chamber temperature to*
348 *evaluate the reversibility of organic nitrate partitioning. The authors attributed all observations as a*
349 *result of gas-particle partitioning, which I think is over-simplifying and not very convincing. I focus my*
350 *comments on Figure 3 here.*

351 *a. First, what is the time series of α-pinene concentration? When the temperature perturbation occurred*
352 *(~240 min), has all the α-pinene reacted? As seen from the figure, during the period between UV off and*
353 *temperature increase, there is still an increase in org/SO₄, which would seem to suggest α-pinene is still*
354 *being reacted and SOA is still being formed? If α-pinene has not all been reacted away, can some of the*
355 *trends we are seeing here a result of on-going reactions?*

356 It is true that some chemistry appears to continue in both the gas and particle phases, although based
357 on the model results the α-pinene has all reacted by this time. However, the primary purpose of this
358 figure is to show that organic nitrates appear to volatilize when temperatures increase, suggesting that
359 the organic nitrates are semi-volatile and their partitioning to the particle phase is reversible. Ozone and
360 NO₂ are present in the chamber during this time, so nitrate radicals can be expected. Some chemistry
361 may continue, but despite this a response in both the particle and gas phase to temperature increase is
362 clearly observed. This has been clarified in the revised manuscript as noted in response to comment #12
363 from Reviewer 1.

364 *b. The authors attributed the increase in gas-phase species as a result of evaporation of these species*
365 *from the particle phase at higher temperatures. In the figure, during the warming period, all the particle*
366 *signals decreased, however, some of the gas-phase signals reached a maximum first and then decreased,*
367 *why? It seems that there is more than gas-partitioning going on here.*

368 Chemistry may continue as gas and particle phase concentrations continue to change slightly without
369 UV light. A potential explanation is that both ozone and nitrate reactions continue to age gas and
370 particle phase compounds. As mentioned in the response to comment a. above the data still show
371 clearly that the particle-phase concentrations respond to an increase in temperature, consistent with
372 semi-volatile species evaporating at higher temperature.

373 *c. At about ~320 min, the temperature decreased. The authors attributed the decrease in gas-phase*
374 *signals to repartitioning of these species to the particle phase. However, the increase in the particle-*
375 *phase concentration is not as substantial (much lower than pre-temperature ramp loading). Why?*

376 When the chamber is cooled the area which will be cold quickest will be the chamber walls. It is not
377 surprising that many gas phase compounds condense to the cold walls of the chamber instead of to
378 particles. The key information in Figure 3 is that when warmed the organic nitrates evaporate from the
379 particle phase. Temperature data (both heating and cooling) is not used in a quantitative way. This has
380 been clarified in the revised manuscript.

381 *d. What is the role of gas-phase wall loss in these observations? One can also argue that the change in*
382 *gas-phase species (in Figure 3c) can be affected by gas-phase wall loss.*

383 We agree, as mentioned in our responses to the above comments.

384 *5. Page 20642 onward, I do not think that the authors can make any definite conclusions regarding*
385 *organic nitrate hydrolysis based on their data.*

386 *a. Line 22. Why did the concentration in Expt 1 continue to increase? Please explain.*

387 In this experiment lower concentrations of α -pinene and hydrogen peroxide delayed and limited the
388 production of SOA. Thus, there was not enough time at the end of the experiment (when OA formation
389 had ceased) to fit an exponential. The data from this experiment were still useful for partitioning
390 calculations, but they were not used to find the nitrate loss rate. This explanation has been updated in
391 the revised manuscript.

392 *b. In determining the rate of decrease in particle-ON, I assume the chamber lights are off? (otherwise*
393 *further photochemical reactions can affect gas and particle-phase composition).*

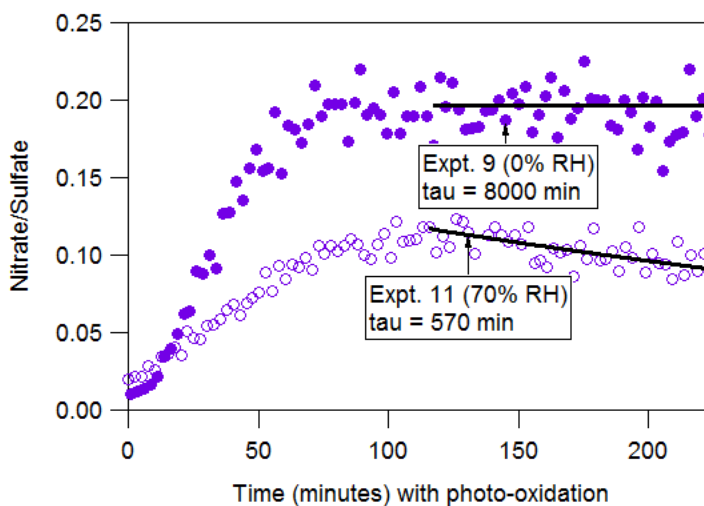
394 The chamber lights were left on during that time period to avoid the formation of NO_3 radical (from NO_2
395 + O_3). While we agree that some further photochemical reactions may have been occurring, during that
396 time period all α -pinene had reacted and the OA composition was not changing significantly (based on
397 f44 signal in the ACSM). With high concentrations of O_3 and NO_2 in the chamber nitrate radicals would
398 form in the dark – which can directly form organic nitrates if double bonds are still present in gas-phase
399 compounds.

400 *c. If the lights are off, are there nitrate radicals in the chamber, are there any further reactions induced*
401 *by the nitrate radicals?*

402 As indicated in our response to 5b above, the lights were left on so nitrate radicals were not expected to
403 be present.

404 *d. The authors need to show the decay (raw data) of the nitrates in the SI, and show clearly how the*
405 *decay rate is determined. e. What does the “decay rate” mean for experiments with RH=0% (Expts 8 and*
406 *9)? Do the authors think that’s also from hydrolysis? If so, where does particle water come from? The*
407 *ammonium sulfate seeds should be solid for a chamber RH of 0%.*

408 Figure S4 has been added to show how this was calculated for experiments – an exponential decay was
409 fit to wall-loss corrected concentrations of organic nitrates and organics. As seen in this figure, even
410 what appears to be a flat line can have a nonzero exponential decay due to scatter in the data. Thus, a
411 fitted/calculated nitrate loss near zero does not necessarily imply hydrolysis was significant or that
412 water was present in the particles.



413

414 Figure S4 – Exponential decay for a low RH (Expt. 9) and high RH (Expt. 11) conditions

415

416 *f. Overall, the authors attributed the decay in nitrates to hydrolysis. To do so, the authors must first*
417 *justify that no other processes or reactions can contribute to the decay of the nitrates (e.g., comments b*
418 *and c, etc)*

419 While it is true that other factors can play a role in the decay of particulate nitrate, the correlation with
420 relative humidity, which follows a similar trend to the work from Liu et al. (2012) is consistent with
421 hydrolysis as the main factor in the observed decay of particulate nitrate. The very low nitrate loss rate
422 at RH below 20% suggests that other factors are minimal in comparison with RH. Other measurements
423 from experiments (organic aerosol concentration, $\cdot\text{OH}$ levels, precursor concentrations) were analyzed
424 for trends with nitrate loss rate but no trends were observed besides that with RH.

425 Ultimately, what we measure are losses of particle-phase organic nitrates. Based on previous work (Liu
426 et al., 2012; Boyd et al., 2015; Rindelaub et al., 2015) the most likely explanation for these particle-phase

427 losses is hydrolysis of the organic nitrates. Neither we nor the previous work observed hydrolysis
428 directly (conversion of the $-\text{ONO}_2$ group to an $-\text{OH}$ group). This has been clarified in the revised
429 manuscript.

430 *g. One way to evaluate hydrolysis rates would be to normalize the decay in nitrates in the humid*
431 *experiments to those in dry experiments, similar to the analysis in Boyd et al. (2015). Have the authors*
432 *look into this?*

433 Since the decay rate at 0% RH is approximately zero this would not change the results significantly.
434 Figure S4 illustrates the difference between exponential decay at high and low RH.

435 *h. What are the uncertainties of the data points shown in Figure 5? Is there supposed to be an increasing*
436 *trend, or the authors think that the loss rate should be constant? Why? Either case, more justifications*
437 *and discussions are needed.*

438 Uncertainties from the ACSM collection efficiency (CE) are not expected to play a role unless CE were to
439 change during the time that the exponential was fit, which is not likely. Wall loss effects are not
440 expected to contribute to uncertainty significantly because the nitrate signal is normalized to sulfate.
441 The uncertainty associated with using the standard fragmentation table (see comment 2e above) would
442 only affect the results if any error introduced by the lack of high resolution data (i.e. the ratio of nitrate
443 mass from high resolution data vs. nitrate mass from low resolution data), changes during the time of
444 the experiment. These changes are expected to be minor during the relatively short time (~ 90 minutes)
445 when the exponential is fit. Based on the variation of measured/fit nitrate loss rate at RH=0% some
446 uncertainty exists. The difference between the measurements of nitrate loss rate at RH=0% (0.6 day^{-1})
447 has been added to the figure as an estimate of uncertainty.

448 *i. The authors noted that Expt 10 is an exception, "possibly due to effects of being near the deliquescence*
449 *relative humidity for that particulate aerosol". Firstly, do the authors mean the DRH for ammonium*
450 *sulfate, or the organic + sulfate aerosol? The DRH for ammonium sulfate is $\sim 80\%$, so at the experiment*
451 *RH of 70%, the ammonium sulfate should be solid? Secondly, the experimental conditions in Expt 10 and*
452 *Expt 11 are very similar, yet the loss rate is drastically different? Why? This goes back to the previous*
453 *comment, what are the uncertainties of the decay rates?*

454 As in response to Reviewer 1, comment #10: An additional experiment was conducted at high (67%) RH
455 and the results warranted additional discussion and an update to Fig. 3 (previously Fig. 5):

456 "Experiments conducted at an average RH of 67% or higher can exhibit a significantly higher decay rate,
457 probably due to effects of being near the deliquescence relative humidity of the ammonium sulfate seed
458 aerosol. In experiments 10 and 12, which have decay rates well above 2 day^{-1} , the chamber was initially
459 cooled to 20°C before the UV lights were turned on. Once the UV lights were activated the temperature
460 then increased to 25°C and the RH settled at the values indicated in Table 1. For these experiments the
461 RH was above 80% (the deliquescence RH, DRH, of $(\text{NH}_4)_2\text{SO}_4$ for several minutes, potentially resulting in
462 aqueous aerosol. Experiment 11 also reached a relative humidity above deliquescence, yet it shows a
463 lower nitrate loss rate than Expts. 10 and 12. The ratio of organics and nitrates to sulfate (seed) particles

464 was much lower in Expt. 11 compared to Expts. 10 and 12, but whether and why this would result in a
465 different nitrate loss rate is currently unclear. The relative humidity in Expt. 4 did not reach the DRH of
466 $(\text{NH}_4)_2\text{SO}_4$. Future work should focus on the fate of ON at higher (> 60%) relative humidity. The generally
467 higher nitrate loss rate at higher RH makes hydrolysis of particulate nitrate functional groups the most
468 plausible explanation for the observed decay.”

469 *j. Page 20643, lines 9-15. The authors need to discuss how the hydrolysis rate determined in this study*
470 *compared to those reported in recent literature. For instance, Rindelaub et al. (2015) studied the*
471 *formation of organic nitrates from photooxidation of α -pinene (same as this study). While Rindelaub et*
472 *al. (2015) did not report a hydrolysis rates for organic nitrates, their results suggested that organic*
473 *nitrates formed from α -pinene+OH+NO_x appear to hydrolyze fairly quickly, which is different from the*
474 *current study? Please discuss. Furthermore, Boyd et al. (2015) reported that majority of the organic*
475 *nitrates formed from β -pinene+NO₃ are primary/secondary nitrates and are stable, while ~10% of the*
476 *organic nitrates are tertiary and hydrolyze on the order of few hours. The hydrolysis rates determined in*
477 *the current study is fairly slow, are the authors implying most of the organic nitrates formed are*
478 *primary/secondary? (this would seem to contradict the results by Rindelaub et al. (2015)?)*

479 The lifetime of particulate ON in this study (12 h) is similar to that measured in two previous studies –
480 Liu et al. 2012 (6 h), Boyd et al. 2015 (3-4.5 h). This discussion has been added to the manuscript as
481 discussed similarly in response to Reviewer 1, comment #5:

482 “No direct observation of hydrolysis (conversion of the -ONO₂ group to an -OH group) has been made in
483 this or previous work. The estimated hydrolysis lifetime of 12 hours (loss rate of 2 day⁻¹) for particulate
484 organic nitrates is similar to hydrolysis rates suggested by other studies under humid conditions. Liu et
485 al. (2012) observed a trend similar to that shown in Fig. 3 in chamber experiments in which ON were
486 formed from the oxidation of tri-methyl benzene using HONO as the ·OH and NO_x source. In those
487 experiments, PM nitrate was found to have negligible loss rate below 20% RH but a lifetime of 6 hours at
488 40% RH and higher. Perring et al. (2009) estimated the lifetime of isoprene nitrates to be between 95
489 minutes and 16 hours depending on their branching ratio in isoprene ·OH oxidation. Boyd et al. (2015)
490 measured a lifetime of 3-4.5 hours for 10% of ON formed from NO₃ oxidation of β -pinene, with a much
491 longer lifetime for the remaining 90%. This suggests that 10% of the ON functional groups were tertiary
492 with the rest being primary or secondary as those have been shown to hydrolyze much slower in the
493 bulk phase (Darer et al., 2011; Hu et al., 2011). In our results hydrolysis is not limited to 10% of ON,
494 suggesting that a higher portion is tertiary ON functional groups.”

495 **References**

496 Ayres, B. R., Allen, H. M., Draper, D. C., Brown, S. S., Wild, R. J., Jimenez, J. L., Day, D. a., Campuzano-Jost,
497 P., Hu, W., de Gouw, J., Koss, a., Cohen, R. C., Duffey, K. C., Romer, P., Baumann, K., Edgerton, E.,
498 Takahama, S., Thornton, J. a., Lee, B. H., Lopez-Hilfiker, F. D., Mohr, C., Goldstein, a. H., Olson, K. and
499 Fry, J. L.: Organic nitrate aerosol formation via NO_x + BVOC in the Southeastern US, Atmos. Chem.
500 Phys. Discuss., 15(12), 16235–16272, doi:10.5194/acpd-15-16235-2015, 2015.

501 Boyd, C. M., Sanchez, J., Xu, L., Eugene, a. J., Nah, T., Tuet, W. Y., Guzman, M. I. and Ng, N. L.: Secondary
502 organic aerosol formation from the β -pinene+NO₃ system: effect of humidity and peroxy radical
503 fate, *Atmos. Chem. Phys.*, 15(13), 7497–7522, doi:10.5194/acp-15-7497-2015, 2015.

504 Chuang, W. K. and Donahue, N. M.: A two-dimensional volatility basis set – Part 3: Prognostic modeling
505 and NO_x dependence, *Atmos. Chem. Phys. Discuss.*, 15(12), 17283–17316, doi:10.5194/acpd-15-
506 17283-2015, 2015.

507 Hilal, S., Karickhoff, S. and Carreira, L.: Prediction of the vapor pressure boiling point, heat of
508 vaporization and diffusion coefficient of organic compounds, *QSAR Comb. Sci.*, 22(6), 565–574,
509 doi:10.1002/qsar.200330812, 2003.

510 Liu, S., Shilling, J. E., Song, C., Hiranuma, N., Zaveri, R. a. and Russell, L. M.: Hydrolysis of Organonitrate
511 Functional Groups in Aerosol Particles, *Aerosol Sci. Technol.*, 46(12), 1359–1369,
512 doi:10.1080/02786826.2012.716175, 2012.

513 Rindelaub, J. D., McAvey, K. M. and Shepson, P. B.: The photochemical production of organic nitrates
514 from α -pinene and loss via acid-dependent particle phase hydrolysis, *Atmos. Environ.*, 100, 193–201,
515 doi:10.1016/j.atmosenv.2014.11.010, 2015.

516 Rollins, a. W., Pusede, S., Wooldridge, P., Min, K.-E., Gentner, D. R., Goldstein, a. H., Liu, S., Day, D. a.,
517 Russell, L. M., Rubitschun, C. L., Surratt, J. D. and Cohen, R. C.: Gas/particle partitioning of total alkyl
518 nitrates observed with TD-LIF in Bakersfield, *J. Geophys. Res. Atmos.*, 118(12), 6651–6662,
519 doi:10.1002/jgrd.50522, 2013.

520 Wildt, J., Mentel, T. F., Kiendler-Scharr, a., Hoffmann, T., Andres, S., Ehn, M., Kleist, E., Müsgen, P.,
521 Rohrer, F., Rudich, Y., Springer, M., Tillmann, R. and Wahner, a.: Suppression of new particle
522 formation from monoterpene oxidation by NO_x, *Atmos. Chem. Phys.*, 14(6), 2789–2804,
523 doi:10.5194/acp-14-2789-2014, 2014.

524

525

526

527 **Other Major Changes in Revised Manuscript**

528

529 In Fig. 2 every 20 data points were averaged for the revised manuscript.

530 In Table 1 the significant figures were decreased on many values.

531

532 **Hydrolysis and Gas-particle Partitioning and Hydrolysis of Organic**
533 **Nitrates Formed from the Oxidation of α -Pinene in Environmental**
534 **Chamber Experiments**

535 **J. K. Bean and L. Hildebrandt Ruiz**

536 McKetta Department of Chemical Engineering, The University of Texas at Austin, Austin, Texas

537 Correspondence to L. Hildebrandt Ruiz (lhr@che.utexas.edu)

538 **Abstract**

539 Gas-particle partitioning and hydrolysis of organic nitrates (ON) influences their role as sinks and sources
540 of NO_x and their effects on the formation of tropospheric ozone and organic aerosol (OA). ~~Organic~~In this
541 work organic nitrates were formed from the photo-oxidation of α -pinene in environmental chamber
542 experiments under ~~varying different~~ conditions. ~~A hydrolysis~~Particle-phase ON hydrolysis rates
543 consistent with observed ON decay exhibited a nonlinear dependence on relative humidity (RH): An ON
544 decay rate of 2 day^{-1} was ~~found for particle-phase ONs at a relative humidity of 22% or higher; observed~~
545 when the RH ranged between 20 and 60%, and no significant ON ~~hydrolysis~~decay was observed at RH
546 lower relative humidity than 20%. In experiments when the highest observed RH exceeded the
547 deliquescence RH of the ammonium sulfate seed aerosol, the particle-phase ON decay rate was as high
548 as 7 day^{-1} and more variable. The ON gas-particle partitioning is dependent on total OA concentration
549 and temperature, consistent with absorptive partitioning theory. In a volatility basis set the ON
550 partitioning is consistent with mass fractions of [0 ~~0.4911~~ ~~0.2903~~ ~~0.5286~~] at saturations mass
551 concentrations (C^*) of [1 10 100 1000] $\mu\text{g m}^{-3}$.

552 **1 Introduction**

553 Organic nitrates (ON) play an important role in atmospheric chemistry as they can act as sinks and
554 sources of NO_x ($\text{NO} + \text{NO}_2$) and thereby affect the formation of tropospheric ozone and organic aerosol.
555 The sink reaction – addition of NO to a peroxy radical ($\text{R-O-O}\cdot$) to form an organic nitrate (R-O-NO_2) –
556 breaks the $\cdot\text{OH}$ initiated oxidation cycle and reduces the formation of ozone (Seinfeld and Pandis, 2006).
557 Most R-O-NO_2 molecules are semi-volatile and are therefore expected to partition between the gas and
558 particle phases. They can be transported in either phase and can become a source of NO_x when they are
559 photolyzed or oxidized, contributing to the regional nature of NO_x pollution. Attempts to implement
560 organic nitrate decomposition reactions in a chemical transport model which did not account for gas-
561 particle partitioning of organic nitrates resulted in over-prediction of NO_x and ozone concentrations
562 (Yarwood et al., 2012), consistent with an over-estimate of the strength of organic nitrates as NO_x
563 sources.

564 Recent studies have suggested that organic nitrates in the condensed phase may undergo hydrolysis,
565 leading to the formation of HNO_3 (Day et al., 2010; Darer et al., 2011; Hu et al., 2011; Liu et al., 2012;
566 Browne et al., 2013; Jacobs et al., 2014; Rindelaub et al., 2015). This is a more permanent sink for NO_x

567 and would decrease the regeneration of NO_x from organic nitrates. While these studies have found
568 evidence for hydrolysis of aerosol-phase organic nitrates (ON^{aer}), it is not clear at which rate ON
569 hydrolysis occurs. Correctly modeling organic nitrates and ozone formation depends on knowledge of
570 the ON partitioning coefficient and hydrolysis rate.

571 While ON hydrolysis in the bulk phase has been studied for decades (Baker and Easty, 1950; Baker and
572 Easty, 1952; Boschan et al., 1955), organic nitrate hydrolysis in atmospheric particles has only recently
573 started to receive attention. Day et al. (2010) observed a decrease in particulate organic nitrates
574 measured in coastal southern California under acidic conditions at high relative humidity and
575 hypothesized hydrolysis as the cause. Browne et al. (2013) used ON hydrolysis to justify observations
576 over the Boreal Forest of higher levels of HNO₃ despite higher production rates of organic nitrates. The
577 chamber experiments (0 to >80% RH) performed by Liu et al. (2012) using trimethylbenzene (an
578 anthropogenic volatile organic compound) and HONO as a precursor oxidant were the first to measure
579 the hydrolysis of condensed organic nitrates. Rindelaub et al. (2015) observed ON hydrolysis while
580 measuring partitioning of α-pinene SOA but did not directly quantify it. Boyd et al. (2015) measured
581 hydrolysis of ON formed from nitrate radical oxidation of β-pinene.

582 The partitioning of organic nitrates to the particle phase is important to determine their fate as only
583 condensed organic nitrates are expected to hydrolyze appreciably to HNO₃. Absorptive partitioning
584 theory (Pankow, 1994; Donahue et al., 2006, Rollins et al., 2013; Rindelaub et al., 2015) has been used
585 to describe the gas-particle partitioning of organic nitrates. Rollins et al. (2013) used partitioning data
586 from the 2010 CalNex Campaign to find a volatility basis set distribution for ON observed at ambient
587 aerosol concentrations. Rindelaub et al. (2015) observed the partitioning of organic nitrates formed
588 from the ·OH initiated oxidation of α-pinene at various levels of relative humidity. However, other work
589 has suggested that the partitioning of organic nitrates to the particle phase is irreversible (Perraud et al.,
590 2012). The goals of this work were to form organic nitrates in controlled environmental chamber
591 experiments from the OH· initiated oxidation of α-pinene under high NO_x conditions and various relative
592 humidity levels and:

- 593 1. Quantify the hydrolysis rate of organic nitrates.
- 594 2. Confirm that the gas-particle partitioning of organic nitrates is reversible and can therefore be
595 modeled by absorptive partitioning theory
- 596 ~~3. Parameterize the gas-particle partitioning of organic nitrates~~
- 597 ~~3. Quantify the hydrolysis rate of organic nitrates.~~

598 2 Methods

599 2.1 Environmental Chamber Experiments

600 All experiments were performed in the Atmospheric Physicochemical Processes Laboratory Experiments
601 (APPLE) chamber located at the University of Texas at Austin (UT-Austin). The APPLE chamber is a ~12

602 m³ Teflon[®] bag suspended inside of a temperature-controlled room. The walls of the room are lined
603 with UV lights which can be used to induce photolysis reactions. The intensity of the UV lights has been
604 characterized by the photolysis rate of NO₂, which was measured to be 0.4 min⁻¹, similar to ~~the expected~~
605 ambient NO₂ photolysis ~~rates~~ (e.g. 0.46 min⁻¹ at a zenith angle of 40°, Carter et al., 2005). Before
606 each experiment the bag was flushed for at least 12 hours with clean air from an Aadco clean air
607 generator (Model 737-14A) at a flow rate exceeding 100 liters per minute (LPM). Ammonium sulfate
608 ((NH₄)₂SO₄) particles (Fisher Scientific, 99.5%) were injected both to monitor wall loss rates (Hildebrandt
609 et al., 2009) as well as to act as seed particles onto which organic vapors can condense. Gas phase NO
610 was injected directly into the chamber from a cylinder (Airgas, 9.94 PPM ±2%) and liquid-phase α-pinene
611 (Sigma Aldrich, 98%) was injected to a glass bulb and subsequently evaporated into the chamber with a
612 steady stream of mildly heated air. H₂O₂, which photolyzes to 2·OH, was used as ·OH radical source and
613 was either injected by bubbling air through an aqueous H₂O₂ solution (Fisher Scientific, 30% weight) or
614 by injecting H₂O₂ solution into a glass bulb and subsequently ~~evaporate~~ ~~evaporating~~ it into the chamber
615 with a steady stream of mildly heated air. Some experiments were performed under dry conditions (<5%
616 relative humidity); in other experiments humidity was increased by passing air through clean water and
617 then into the chamber. Experimental conditions and results are summarized in Table 1. Results are
618 discussed in Sect. 3.

619 Reactions were allowed to proceed for at least 4 hours with continuous UV light. Experiments were run
620 in a batch mode with no injections or dilution after the experiment was started; the bag volume of 12
621 m³ allowed ample time for sampling. In some cases the temperature effects on gas-particle partitioning
622 were observed by increasing temperature to 40 °C in the chamber after the UV lights had been turned
623 off (see Sect. 3.2).

624

625 2.1.1 Instrumentation

626 The composition of PM₁ (particulate matter smaller than 1 micrometer in diameter) was measured using
627 an Aerosol Chemical Speciation Monitor (ACSM) from Aerodyne ~~Research Inc.~~ (Ng et al., 2011). In the
628 ACSM, particles are flash-vaporized on a heater at 600 °C, and the resulting gas molecules are ~~then~~
629 ionized using electron-impact ionization. This harsh ionization method results in fragmentation of most
630 molecules. The molecular fragments, which are measured by a quadrupole mass spectrometer, are
631 attributed to four categories—organics, nitrate, sulfate, and ammonium - using a fragmentation table
632 (Allan et al., 2004). The instrument alternates between normal sampling and sampling through a particle
633 filter, enabling subtraction of a gas-phase background. During this study the ACSM was operated at a
634 time resolution (filter/sample cycle length) of approximately 90 seconds. The size distribution of
635 particles was measured using a Scanning Electrical Mobility System (SEMS) from Brechtel
636 Manufacturing, Inc. The SEMS uses a Differential Mobility Analyzer (DMA) to size-select particles based
637 on their electric mobility, which are then counted by a Condensation Particle Counter (CPC). The DMA
638 continuously cycled between the voltages which select particles ranging from 5 to 1000 nm, resulting in
639 a time resolution of the particle size distribution of approximately 60 seconds.

640 Gas phase reaction products were monitored using a High-Resolution Time-of-Flight Chemical Ionization
641 Mass Spectrometer (HR-ToF-CIMS) from Aerodyne Research, Inc.. The HR-ToF-CIMS uses softer chemical
642 ionization which results in minimal fragmentation of parent molecules. Mass spectra are derived from
643 measurements of the ions' time-of-flight as they are pulsed through a low pressure chamber in a "V"
644 shape. Two chemical reagent ions were used—water clusters ($\text{H}_3\text{O}^+(\text{H}_2\text{O})_n$) and iodide-water clusters (I^-
645 $\cdot(\text{H}_2\text{O})_n$). Water cluster ionization is most sensitive towards detection of moderately oxidized
646 hydrocarbons; the ability to ionize and thus sensitivity is based on the relative proton affinity between
647 the water cluster and the parent molecule (Lindinger et al., 1998). This method was used to monitor α -
648 pinene as well as early-generation oxidation products. Iodide-water cluster ionization is most sensitive
649 towards detection of more highly oxidized hydrocarbons; this method was used to observe later-
650 generation oxidation products as well as HNO_3 and H_2O_2 . In the work presented here data from the HR-
651 ToF-CIMS are only used qualitatively since, as it was later discovered, a partially clogged inlet may have
652 interfered with instrument calibration and quantitative measurements.

653 Concentrations of NO and O_3 were measured using Teledyne chemiluminescence NO_x and absorption O_3
654 monitors (200E and 400E, respectively); concentrations of NO_2 were measured via an NO_2 monitor from
655 Environnement (Model AS32M), which uses a Cavity Attenuated Phase Shift (CAPS) method to directly
656 measure NO_2 (Kebabian et al., 2008). The advantage of this direct NO_2 measurement is that it does not
657 rely on NO_2 conversion to NO and therefore does not suffer from interference by other oxidized
658 nitrogen compounds such as HONO and organic nitrates (Winer et al., 1974).

659 2.1.2 Data Analysis

660 Data from the ACSM were analyzed in Igor Pro using the software package "ACSM Local," which includes
661 a correction for relative ion transmission efficiency as well as changes in the flow rate throughout the
662 experiment. The SEMS volume concentration was converted to mass using the densities 1.77 g/cm^3 for
663 ammonium sulfate and 1.4 g/cm^3 for organics and organic nitrates (Ng et al., 2007). The time series of
664 particle mass concentration (not corrected for wall losses) during Expt. 7 is shown in Fig. S1; other
665 experiments exhibited similar time series.

666 All PM nitrate (measured by the ACSM as NO^+ and NO_2^+ fragments) was assumed to be organic because
667 no inorganic nitrate was introduced in these controlled experiments. Nitric acid is formed in the gas
668 phase as well as in the particle phase through hydrolysis as well as in the gas phase, but it is assumed
669 that nitric acid concentrations are negligible in the particle phase due to its high vapor pressure (Fry et
670 al., 2009). A Henry's Law calculation suggests that the total amount of aqueous HNO_3 in particles is 3
671 orders of magnitude lower than that in the gas phase.

672 The ACSM does not detect all sampled particles, primarily due to particle bounce at the vaporizer,
673 resulting in a collection efficiency (CE) smaller than 1. Collection efficiency and wall losses were
674 accounted for simultaneously by multiplying the ACSM concentrations of organics and organic nitrates
675 by the mass concentration ratio $C_{SEMS}^{t=0}/C_{ACSM}^{seed}(t)$ as has been done in previous work (Hildebrandt et al.,
676 2009). Here, $C_{SEMS}^{t=0}$ is the mass concentration of ammonium sulfate seed just before the UV lights are
677 turned on and organic aerosol formation commences and $C_{ACSM}^{seed}(t)$ is the time dependent mass

678 concentration of $(\text{NH}_4)_2\text{SO}_4$ measured by the ACSM throughout the experiment. This correction assumes
679 that particles on the chamber walls participate in gas-particle partitioning as though they are still in
680 suspension and that the suspended ammonium sulfate concentration changes only due to wall losses. It
681 accounts for partitioning of organic vapors into wall-deposited particles (Hildebrandt et al., 2009) but
682 does not account for losses of organic vapors onto the clean Teflon® walls (e.g. Matsunaga and Ziemann,
683 2010).

684 The ACSM standard fragmentation table was adjusted based on filter measurements taken in each
685 experiment as described in the supplementary information. Data from the HR-ToF-CIMS were analyzed
686 in Igor Pro (Wavemetrics) using Tofware, the software provided with the instrument. The data were first
687 mass calibrated based on HR-ToF-CIMS reagent ions and other known ions. The baseline was subtracted
688 and the average peak shape was found so it could be used for high resolution analysis, through which
689 multiple ions can be identified at any given integer m/z . Ions up to m/z 300 were analyzed in high
690 resolution mode. Only prominent ions were fit above m/z 200 because of the high number of possible
691 ions at this high m/z . After ions were identified in the high resolution spectrum, the peaks were
692 integrated to yield a time series of ions. Analyte ion concentrations were then normalized by the
693 reagent ion concentrations – the sum of H_3O^+ , $\text{H}_3\text{O}^+\cdot(\text{H}_2\text{O})$ and $\text{H}_3\text{O}^+\cdot(\text{H}_2\text{O})_2$ for water cluster
694 ionization and the sum of I^- and $\text{I}^-\cdot(\text{H}_2\text{O})$ for iodide-cluster ionization. This correction accounts for
695 changes in reagent ion concentrations and instrument sensitivity during and between experiments.
696 Relative humidity can affect instrument sensitivity but this varied by less than 5% during each
697 experiment.

698 The partitioning coefficient of a species is defined as the ratio of the species concentration in the
699 particle phase to the total species concentration (gas and particle phase). For a single compound the
700 partitioning coefficient is the same whether it is on a mass or mole basis. However, for a mix of
701 compounds, such as those formed in $\cdot\text{OH}$ -initiated oxidation, the mass and mole-basis partitioning
702 coefficients will be different, with the coefficient expected higher on a mass basis since higher molecular
703 weight compounds typically have lower vapor pressure. The partitioning coefficient in this work was
704 calculated on a mole basis, in part because fragmentation in the ACSM makes it impossible to tell the
705 original size and identity of ON molecules. This mole-basis partitioning coefficient is also more useful for
706 most modeling efforts which group chemical species without knowledge of their exact molecular
707 identity. The particle-phase ON concentration was quantified using data from the ACSM: the mass
708 concentrationsconcentration of NO^+ and NO_2^+ fragments-nitrate measured by the ACSM were
709 converted to mixing ratiosratio (ppb) using the molecular weightsweight of the fragments, and the sum
710 of the PM- NO^+ and NO_2^+ mixing ratios was used as the ON mixing ratio-nitrate functional group (62
711 g/mol). This assumes that the ON have only one nitrate functional group. Conversion of the NO^+ and
712 NO_2^+ nitrate mass concentrationsconcentration to mixing ratiosratio avoids the need to assume an ON
713 molecular weight (needed to estimated ON mass concentrations from ACSM) and is therefore deemed
714 to be a more accurate measure of ON from the ACSM. Quantification of all gas phase ON species would
715 necessitate calibration and identification of all ON species which is not feasible. Instead, a chamber box
716 model and nitrogen balance was employed to estimate total gas-phase ON as described below.

717 2.2 Chamber Modeling and Partitioning Coefficient

718 In these experiments only five major forms of oxidized nitrogen are present in significant
719 concentrations—NO, NO₂, HNO₃, ON^{gas} and ON^{aer} (gas and aerosol-phase organic nitrates, respectively).
720 Figure S2 shows that, based on the Statewide Air Pollution Research Center (SAPRC) model
721 (<http://www.engr.ucr.edu/~carter/SAPRC/>), the concentrations of other forms of reactive nitrogen are
722 orders of magnitude lower than the concentrations of these five forms. Concentrations of NO and NO₂
723 were measured using gas-phase monitors, and ON^{aer} was measured using the ACSM. Concentrations of
724 HNO₃ were approximated using the Statewide Air Pollution Research Center (SAPRC) box model
725 (<http://www.engr.ucr.edu/~carter/SAPRC/>). The SAPRC box model. The concentration of H₂O₂ cannot be
726 estimated from the injection method used in these experiments. Therefore, the H₂O₂ concentration
727 used in the model was adjusted until the modeled NO, NO₂, and O₃ concentrations closely matched
728 those observed throughout each experiment as shown in Fig. S2S3 for Expt. 7. The modeled HNO₃
729 concentration was then used with the measured NO, NO₂, and ON^{aer} to find the ON^{gas} based on a
730 nitrogen mass balance (ON^{gas} = NOX^{initial} - NO₂ - NO - ON^{aer} - HNO₃^{model}). The partitioning coefficient
731 (ON^{aer} / ON^{aer} + ON^{gas}) was then calculated as a time series for each experiment.

732 SAPRC simulations were conducted with the reaction mechanism Carbon Bond 6 revision 2 (CB6r2),
733 which includes organic nitrate hydrolysis through a rate estimated from a combination of the work of Liu
734 et al. (2012) and Rollins et al. (2013) (Hildebrandt Ruiz and Yarwood, 2013). Experiments were modeled
735 with and without organic nitrate hydrolysis to see the effect this has on the predicted ON partitioning
736 coefficient. The overall effect of this process in the model was small: in 80% of the data points used
737 (individual time points from each experiment) to find the volatility basis set (described below) the
738 removal of the hydrolysis process in the model causes, with a maximum effect being a 5% decrease into
739 the calculated partitioning coefficient of less than 5%. The maximum decrease in partitioning coefficient
740 (8.6%) due to removal of the modeled hydrolysis process by removing the hydrolysis mechanism from
741 the model. This corresponded to a 17% decrease in HNO₃ of 27% at that particular time. This shows,
742 which suggests that the partitioning coefficient estimated in this work is not very sensitive to changes in
743 the modeled HNO₃ concentrations. For the results and analysis presented here the HNO₃ concentrations
744 were taken from CB6r2 with the inclusion of the ON hydrolysis process for experiments above 20% RH
745 and without the hydrolysis process for experiments below 20% RH.

746 According to absorptive partitioning theory (Pankow, 1994; Donahue et al., 2006), the gas-particle
747 partitioning of an organic species depends on its vapor pressure and the concentration of organic
748 material already in the condensed particle phase. The fraction of a compound *i* in the particle phase (*Y_i*)
749 is given by (Donahue et al., 2006):

$$750 \quad Y_i = \left(1 + \frac{C_i^*}{C_{OA}}\right)^{-1} \quad (1)$$

751 where *C_{OA}* is the organic aerosol concentration and *C_i^{*}* is the saturation mass concentration of species *i*
752 (the saturation vapor pressure converted to concentration units). In the volatility basis set (VBS,
753 Donahue et al., 2006), organic species are lumped by *C_i^{*}* spaced logarithmically. This leads to an overall
754 partitioning coefficient

755
$$Y_{tot} = \sum_{i=1}^n F_i \left(1 + \frac{C_i^*}{C_{OA}}\right)^{-1} \quad (2)$$

756 (Rollins et al., 2013), where F_i is the fraction of organic species in the volatility bin described by C_i^* . In
757 this work we used measurements of C_{OA} and Y_{tot} to fit the F_i using a Matlab optimization routine. These
758 VBS parameters can be used in models to represent the gas-particle partitioning of organic nitrates and
759 account for changes in partitioning with temperature and C_{OA} .

760 3 Results and Discussion

761 A typical time series of compounds containing oxidized nitrogen is shown in Fig. 1 (Expt. 7). Initially the
762 chamber contains only NO and a small amount of NO₂, in addition to α -pinene and inorganic seed
763 aerosol. When the UV lights are activated at time = 0 the NO immediately begins to react with ·OH and
764 other radicals to form NO₂ and additional NO_y compounds such as organic nitrates. ~~Concentrations of
765 ON^{aer} and ON^{gas} from all experiments are summarized in Table 1. Table 1 summarizes results from all
766 experiments. Concentrations of O₃, ON^{aer}, PM organics, and ON^{gas} are averaged over approximately 20
767 minutes of the time when PM organics and nitrates peak in concentration. This averaging period was
768 chosen so that experiments with different H₂O₂ concentrations could be compared even though they
769 reach their maximum concentrations at different rates. Higher initial loading of NO_x, α -pinene, and H₂O₂
770 resulted in higher concentrations of ozone and PM.~~

~~In high RH experiments (Expts 4, 10 and 11) ON^{gas} concentrations calculated using this mass balance
771 approach are very low and sometimes below zero. This could be caused by an overestimate of wall-loss
772 corrected ON^{aer} concentrations at high relative humidity. The wall-loss correction used here and in
773 previous work (Hildebrandt et al., 2009) assumes that particles lost to the walls still participate in
774 partitioning as though in suspension. This assumption may be poor if small amounts of water condense
775 onto the walls of the chamber in high RH experiments. It is also possible that at high relative humidity
776 HNO₃ partitions to the particle phase and is measured by the ACSM. In this case it would be double
777 counted in the mass balance as both HNO₃ and as ON^{aer}, which would lower the estimates for ON^{gas}. Due
778 to these issues with calculating the gas-phase ON concentrations in high RH experiments only low RH
779 experiments are used for calculating the ON partitioning coefficient.~~

781 Figure 2 shows time series of ~~selected~~ molecular ions identified using the HR-ToF-CIMS using water
782 cluster (“positive mode”) and iodide-water cluster (“negative mode”) ionization. ~~Many compounds are
783 identified with the CIMS and a select few of the most prominent compounds were chosen for Fig. 2. In
784 short time periods after switching reagent ions the sensitivity of the HR-ToF-CIMS slowly adjusts to a
785 steady state value. Minor changes during these short time periods should be taken with caution but the
786 overall trends over the 4.5 hour experiment are useful in viewing oxidation trends.~~ The initial data
787 collected in negative mode show that formation of organic nitrates begins immediately after oxidation
788 has started. ~~The~~ Later in the experiment the less-oxygenated compounds observed in positive mode
789 begin to decrease while the more highly oxygenated compounds observed in negative mode continue to
790 increase, consistent with oxidation and conversion of less-oxidized compounds to more highly-oxidized
791 compounds continuing throughout the experiment. Highly-oxidized compounds which still contain ten

792 carbon atoms (as the precursor α -pinene) begin to decrease towards the end of the experiment while
793 fragmented ~~compound~~compounds (containing less than ten carbon atoms) continue to increase,
794 consistent with fragmentation of the carbon backbone during oxidation. Molecular weights of the gas-
795 phase compounds identified here range from 221 to 279 g mol⁻¹ and align well with the range of
796 molecular weights estimated by Fry et al. (2009) for particle-phase organic nitrates formed from NO₃
797 oxidation of α -pinene (229±12 to 434±25 g mol⁻¹). Gas-phase organic nitrates identified here are
798 therefore expected to be semi-volatile and to partition significantly to the particle phase.

799 **3.21 Hydrolysis of Organic Nitrates**

800 Concentrations of wall-loss corrected (normalized to SO₄) PM ~~organics and~~ nitrate were observed to
801 decrease towardsat the end of most experiments. ~~(The exception was experiment 1, in which~~
802 ~~concentrations continued to increase.)~~ These decreases of PM ~~organics and~~ PM-nitrate are attributed to
803 physical or chemical processes in the gas and aerosol phases, and an exponential decay was fit to the
804 data to quantify the decay. ~~A correlation is observed between the rate of this decay for PM nitrate and~~
805 ~~the~~ The exception was experiments 1 and 3 during which production of SOA was slow (primarily due to
806 lower initial H₂O₂ and α -pinene) and continued throughout the experiment, so a decay could not be
807 observed. Examples of the decay for a humid and dry experiment are shown in Fig. S4. The decay rates
808 for each experiment are reported in Table 1 and appear to depend on relative humidity as shown in Fig.
809 5. The details for each experiment are found in table 1. In 3. When the four experiments with RH ranged
810 between 20 and 60%, an RH at 15% or below there appears to be little or ON decay rate of 2 day⁻¹ was
811 observed; no disappearance of nitrate. However, for experiments with significant ON decay was
812 observed at RH at 22% and lower than 20%. Experiments conducted at an average RH of 67% or higher
813 the nitrate loss rate is approximately 2 day⁻¹. The one exception to this is Expt. 10 (RH = 70%), which
814 exhibitedcan exhibit a significantly higher decay rate, ~~possibly~~probably due to effects of being near the
815 deliquescence relative humidity for that particular of the ammonium sulfate seed aerosol.

816 MeasuringIn experiments 10 and 12, which have decay rates well above 2 day⁻¹, the ~~disappearance of~~
817 ~~nitrate with~~chamber was initially cooled to 20 °C before the ACSM assumes that HNO₃ formed through
818 hydrolysis volatilizes, consistent with its high-vapor pressure (Fry et al., 2009). If HNO₃ does not volatilize
819 completely, this method UV lights were turned on. Once the UV lights were activated the temperature
820 then increased to 25 °C and the RH settled at the values indicated in Table 1. For these experiments the
821 RH was above 80% (the deliquescence RH, DRH, of (NH₄)₂SO₄ for several minutes, potentially resulting in
822 aqueous aerosol. Experiment 11 also reached a relative humidity above deliquescence, yet it shows a
823 lower nitrate loss rate than Expts. 10 and 12. The ratio of organics and nitrates to sulfate (seed) particles
824 was much lower in Expt. 11 compared to Expts. 10 and 12, but whether and why this would result in an
825 underestimate of the ON hydrolysisa different nitrate loss rate is currently unclear. The relative humidity
826 in Expt. 4 did not reach the DRH of (NH₄)₂SO₄. Future work should focus on the fate of ON at higher (>
827 60%) relative humidity. The generally higher nitrate loss rate at higher RH makes hydrolysis of
828 particulate nitrate functional groups the most plausible explanation for the observed decay.

829 ~~These results are consistent with other studies of the PM organics also decreased in some experiments,~~
830 ~~but their loss rate was lower and more variable than that of nitrate. Based on the work by Chuang et al.~~
831 ~~(2015) the addition of a nitrate functional group decreases volatility of a compound by 2.5 orders of~~

832 magnitude – slightly more than the resulting alcohol group from hydrolysis. Thus, the organic
833 nitrate compound resulting from ON is more volatile than the original organic nitrate, and as a result
834 could partition to the gas phase, resulting in a decrease in PM organics.

835 No direct observation of hydrolysis rate (conversion of the -ONO₂ group to an -OH group) has been
836 made in this or previous work. The estimated hydrolysis lifetime of 12 hours (loss rate of 2 day⁻¹) for
837 particulate organic nitrates is similar to hydrolysis rates suggested by other studies under humid
838 conditions. Liu et al. (2012) observed a trend similar to that shown in Fig. 53 in chamber experiments in
839 which ON were formed ~~through~~ from the oxidation of tri-methyl benzene using HONO as the ·OH and
840 NO_x source. In those experiments, PM nitrate was found to have negligible loss rate below 20% RH
841 ~~and but~~ a ~~loss rate~~ lifetime of 4 day⁻¹ 6 hours at 40% RH and higher. Perring et al. (2009) estimated the
842 lifetime of isoprene nitrates to be between 95 ~~min and 16 hrs based on their branching ratio in isoprene~~
843 ~~·OH oxidation minutes and 16 hours depending on their branching ratio in isoprene ·OH oxidation.~~ Boyd
844 et al. (2015) measured a lifetime of 3-4.5 hours for 10% of ON formed from NO₃ oxidation of β-pinene,
845 with a much longer lifetime for the remaining 90%. This suggests that 10% of the ON functional groups
846 were tertiary with the rest being primary or secondary as those have been shown to hydrolyze much
847 slower in the bulk phase (Darer et al., 2011; Hu et al., 2011). In our results hydrolysis is not limited to
848 10% of ON, suggesting that a higher portion is tertiary ON functional groups.

849 Similar VOC precursors such as α-pinene and β-pinene can form different fractions of primary/secondary
850 and tertiary ON. When NO₃ reacts and bonds with the terminal double bond of β-pinene, an alkyl radical
851 is formed in either a primary or tertiary position (opposite of the carbon-nitrate bond). The tertiary alkyl
852 radical is more stable, so primary organic nitrates are expected to be more abundant. The double bond
853 in α-pinene is not terminal, so the NO₃ reaction produces either a secondary or tertiary ON and alkyl
854 radical. NO₃ typically bonds with the less substituted carbon of a double bond so that a more highly
855 substituted alkyl radical is formed. The reverse is true for OH+NO chemistry. In this case NO reacts with
856 the peroxy-radical to form the nitrate group. The peroxy-radical, a product of O₂ and an alkyl radical, is
857 likely to be on a more substituted carbon as this would have been the more stable alkyl radical. Thus,
858 more highly substituted ON are expected from OH + NO_x than from NO₃ chemistry. This has important
859 implications for attempts to model ON and the resulting NO_x recycling.

860 As Table 1 shows, ~~we conducted~~ experiments were conducted at varying NO_x and α-pinene
861 concentrations, relative humidity, and hydrogen peroxide (·OH radical source) levels, which resulted in
862 different final concentrations of PM nitrate and total OA. Liu et al. (2012) suggested that a lower PM
863 nitrate / OA ratio at higher RH could be due to ON hydrolysis. In these experiments, the correlation
864 between the ratio of PM nitrate/total OA (measured when total OA was highest) and RH was very low
865 (R² = 0.02). Thus, based on these experiments, differences in the observed final PM nitrate / OA ~~could~~
866 ~~beare~~ due to experimental conditions other than relative humidity.

867 **3.12 Gas-particle Partitioning of Organic Nitrates**

868 In order to test the reversibility of ON partitioning the temperature of the chamber was increased after
869 OA had formed (and when the UV lights were off) in some experiments. Figure 34 shows gas and
870 particle-phase measurements taken from a representative experiment (Expt. 2). After the UV lights are

871 turned off there is a 60 minute period in which the temperature stabilizes around 15 °C. This is followed
872 by ~90 minutes of heating to a final temperature of 45 °C. After this the chamber is quickly cooled back
873 to 15 °C. Figure [3b4b](#) shows a time series of the Org/SO₄ and ON^{aer}/SO₄ ratios measured by the ACSM.
874 Sulfate has a low vapor pressure and does not evaporate significantly at the temperatures investigated;
875 therefore changes in the ON^{aer}/SO₄ and Org/SO₄ ratios with chamber temperature can be attributed to
876 partitioning of organic nitrates and other organic species between the gas and particle phases- or wall
877 losses of gas-phase species. As Fig. [3b4b](#) shows, Org/SO₄ and ON^{aer}/SO₄ decreased with increasing
878 temperature and increased with decreasing temperature, suggesting evaporation of species at higher
879 temperatures and their re-partitioning to the particle phase at lower temperatures.

880 Figure [3b4c](#) shows the effects of temperature on various compounds measured in the gas phase. Several
881 organic compounds – with and without ON functional groups - increase with increasing temperature.
882 This suggests that these compounds are present in both the gas and particle phases and evaporate at
883 higher temperature resulting in increased gas phase concentrations. As temperature is increased the
884 percent change in the concentration of gas-phase C₁₀H₁₆O₂ is less than the change in C₁₀H₁₆O₄ and the
885 percent change in the concentration of gas-phase C₁₀H₁₅NO₄ is less than the change in C₁₀H₁₅NO₆. This is
886 consistent with the more highly oxidized compounds having a lower vapor pressure and evaporating
887 less. As the temperature is decreased back to 15 °C the concentrations return to the pre-heating trends,
888 suggesting that re-condensation to the particle-phase has occurred. These observations, as well as the
889 trends seen in particle-phase measurements are consistent with equilibrium partitioning and
890 inconsistent with the irreversible partitioning of ON recently suggested by Perraud et al. (2012).

891 Other processes may influence particle and gas concentrations of organic compounds. Continuing
892 reactions with O₃ and nitrate radicals (since O₃ and NO₂ are both present) limit the ability to stop all
893 chemical activity. This is seen in the gas phase compounds, some of which appear to be changing in
894 concentration after the UV lights are off. Despite this a clear change is seen in all compounds with a
895 temperature increase. During the cooling phase (beginning at t = 320 minutes) the particle phase
896 organic and nitrate concentrations do not return to the original levels. It is likely that some organic
897 compounds are lost to the walls of the Teflon chamber, especially since they reach the coldest
898 temperatures during active cooling, and thus Org/SO₄ does not return to the values seen before
899 temperature changes began. Despite these limitations it is clear that both the Org/SO₄ and ON^{aer}/SO₄
900 ratios decrease with heating, consistent with semi-volatile organics and organic nitrates.

901 Table 1 summarizes results from all experiments. Each value in the table is an average the ON
902 partitioning coefficient averaged over approximately 20 minutes of the time from when PM organics and
903 nitrates peak in concentration. We chose to compare the data at the maximum so that Partitioning data
904 is not calculated for experiments above 60% RH. As discussed, these experiments with different H₂O₂
905 concentrations could be compared even had higher and less consistent nitrate decay rates which may
906 affect partitioning. In addition, the wall loss correction used here and in previous work (Hildebrandt et
907 al., 2009) assumes that particles lost to the walls still participate in partitioning as though they reach
908 their maximum concentrations at different rates. Higher initial loading of NO_x, α-pinene, and H₂O₂
909 results in higher ozone and PM concentrations. The average partitioning coefficient of ON for this time
910 period in each experiment is also shown; a more detailed analysis were still in suspension. This

911 ~~assumption may be poor if small amounts of ON partitioning follows. As mentioned above gas-phase ON~~
912 ~~could not be estimated reliably for water condense onto the walls of the chamber in these high RH~~
913 ~~experiments, and therefore Table 1 only shows partitioning coefficients for low RH experiments.~~

914 Data from the lower-concentration experiments (Expts 1, 2, and 3) were fit to a volatility basis set as
915 these experiments were conducted under conditions which are more atmospherically relevant
916 conditions. Experimental data were used after total PM organics (corrected for wall losses) had reached
917 $2 \mu\text{g m}^{-3}$ to avoid effects of noise and model uncertainty at the beginning of the experiments when
918 concentrations of both gas- and particle-phase organic nitrates were low. Outlying points (for example,
919 when PM organics temporarily ~~jumped to rose~~ above $2 \mu\text{g m}^{-3}$ but subsequent data suggested that
920 condensation had not begun) were removed as well. Figure 4a5 shows the data used to find the
921 volatility basis set along with the fit. The C^* values used for this were 1, 10, 100, and $1000 \mu\text{g m}^{-3}$; the
922 corresponding mass fractions (F_i) calculated to give the best fit for Eq. (2) (Sect. 2.2) are $F_i = 0, 0.1911,$
923 $0.2903,$ and 0.5286 .

924 ~~The data from higher concentration experiments (Expts 5-9) is shown with the volatility basis set trace~~
925 ~~seen in Fig. 4b. The data selected are those from the time period from when the NOx monitor reading of~~
926 ~~NO was first below 5 ppb to ten minutes after the peak of the corrected PM nitrate signal. The NO~~
927 ~~concentration of below 5 ppb was chosen to minimize any hysteresis effects of the NO monitor on the~~
928 ~~mass balance calculation of the partitioning coefficient (time delays in measurements were observed~~
929 ~~during calibrations of the Teledyne NOx monitor). This was not needed for low concentration~~
930 ~~experiments because they were conducted with low H₂O₂ levels and slower resulting rates—minimizing~~
931 ~~the effects of hysteresis from the NOx monitor. Data were only used up to the time of 10 minutes after~~
932 ~~the peak of PM nitrate to minimize effects of uncertainty in the wall loss correction, which increase over~~
933 ~~the course of an experiment. There is good agreement between the data points from these experiments~~
934 ~~and the volatility basis set which was found from only the lower concentration experiments.~~

935 ~~These~~ these results indicate that under typical ambient conditions ($< 40 \mu\text{g m}^{-3}$ of OA) 5-20%
936 partitioning of ON is expected. 10% of organic nitrates formed from the photo-oxidation of α -pinene
937 under high NOx conditions are expected to partition to the particle phase. This is significantly lower than
938 the organic nitrate partitioning ~~coefficient~~ calculated by RollingsRollins et al. (2013) for organic nitrates
939 measured in Bakersfield, CA during the CalNex campaign in 2010 ~~as shown in Fig. 4.~~ In those
940 measurements >30% partitioning of ON was observed at organic aerosol concentrations of $10 \mu\text{g m}^{-3}$.
941 The difference could be attributed to differences in precursor molecules and levels of oxidation. Studies
942 have shown that high NOx conditions can shift photochemical oxidation products of terpenes towards
943 higher volatility compounds (Wildt et al. 2014). Rollins et al. determined using the SPARC model (Hilal et al., 2003) that precursor molecules (a mix of C5-C15 VOCs) would need two stages of oxidative
944 chemistry beyond the initial ~~-OH +~~ oxidation of the VOC to reach the point when ~~they~~ 19-28% would
945 partition at 19-28% to the particle phase for a C_{OA} of $3 \mu\text{g m}^{-3}$. ~~Our chamber data using α -pinene as a~~
946 ~~precursor appears to be m^{-3} .~~ This may suggest that the ON formed in our experiments have undergone
947 fewer than three generations of oxidation as they are more volatile than ~~that the ON~~ measured in
948 Bakersfield during CalNex 2010. It should also be noted that the thermal dissociation-laser induced
949 fluorescence (TD-LIF) instrument used by Rollins et al. (2013) has been shown in a recent study to

951 [measure PM ON a factor of two higher than the ON measured by aerosol mass spectrometers \(Ayres et](#)
952 [al., 2015\) which utilize similar measurement and detection techniques as the ACSM used in this work.](#)
953 [While the reasons for this difference are unknown it would result in a higher partitioning coefficient](#)
954 [compared to the one calculated from the AMS \(or ACSM\) and explain part of the observed difference.](#)

955 4 Conclusions

956 ~~We give evidence that organic~~ [Organic](#) nitrates formed during the oxidation of α -pinene ~~are~~
957 ~~hydrolyzed~~ [decay](#) in the particle phase at a rate of 2 day^{-1} when RH is ~~22% or higher~~ [between 20 and](#)
958 [60%, with no significant decay observed below an RH of 20%. During experiments when the highest](#)
959 [observed RH exceeded the deliquescence RH of the ammonium sulfate seed aerosol, the particle-phase](#)
960 [ON decay was as high as \$7 \text{ day}^{-1}\$ and more variable. The dependence of observed decay rate on relative](#)
961 [humidity suggests organic nitrate hydrolysis as the most plausible explanation.](#) The gas-particle
962 partitioning of ON determines their potential to hydrolyze. ~~We find that partitioning~~ [Partitioning](#) of the
963 ON is reversible and can be described by a volatility basis set ~~where the mass fractions at saturation~~
964 ~~mass concentrations of 1, 10, 100, and $1000 \mu\text{g m}^{-3}$ are 0, 0.190, 0.275, and 0.535, respectively.~~

965 The conversion of NO_x to organic nitrates affects local ozone production. Partitioning and hydrolysis of
966 organic nitrates affect regional concentrations of organic particulate matter and ozone. The organic
967 nitrate partitioning coefficient and hydrolysis ~~rate~~ [rates](#) from this work can be used to include these
968 processes in chemical transport models and more accurately represent the effect of organic nitrates on
969 concentrations of ozone and particulate matter.

970 5 Acknowledgements

971 This work was financed in part through a grant from the Texas Commission on Environmental Quality
972 (TCEQ), administered by The University of Texas through the Air Quality Research Program (Project 12-
973 012). The contents, findings opinions and conclusions are the work of the authors and do not
974 necessarily represent findings, opinions or conclusions of the TCEQ. The work was also financed in part
975 through a grant by the Texas Air Research Center (Project 312UTA0132A).

976 6 References

977
978 Allan, J. D., Delia, A. E., Coe, H., Bower, K. N., Alfarra, M. R., Jimenez, J. L., Middlebrook, A. M., Drewnick,
979 F., Onasch, T. B., Canagaratna, M. R., Jayne, J. T. and Worsnop, D. R.: A generalised method for the
980 extraction of chemically resolved mass spectra from Aerodyne aerosol mass spectrometer data, J.
981 Aerosol Sci., 35(7), 909–922, doi:10.1016/j.jaerosci.2004.02.007, 2004.

982 [Ayres, B. R., Allen, H. M., Draper, D. C., Brown, S. S., Wild, R. J., Jimenez, J. L., Day, D. A., Campuzano-](#)
983 [Jost, P., Hu, W., de Gouw, J., Koss, A., Cohen, R. C., Duffey, K. C., Romer, P., Baumann, K., Edgerton,](#)
984 [E., Takahama, S., Thornton, J. A., Lee, B. H., Lopez-Hilfiker, F. D., Mohr, C., Goldstein, A. H., Olson, K.](#)
985 [and Fry, J. L.: Organic nitrate aerosol formation via NO_x + BVOC in the Southeastern US, Atmos.](#)
986 [Chem. Phys. Discuss., 15\(12\), 16235–16272, doi:10.5194/acpd-15-16235-2015, 2015.](#)

- 987 Baker, J. and Easty, D.: Hydrolysis of Organic Nitrates, *Nature*, 166(4212), 156–156,
988 doi:10.1038/166156a0, 1950.
- 989 Baker, J. and Easty, D.: Hydrolytic Decomposition of Esters of Nitric Acid .1. General Experimental
990 Techniques - Alkaline Hydrolysis and Neutral Solvolysis of Methyl, Ethyl, Isopropyl, and Tert-Butyl
991 Nitrates in Aqueous Alcohol, *J. Chem. Soc.*, (APR), 1193–1207, doi:10.1039/jr9520001193, 1952.
- 992 Boschan, R., Merrow, R. T. and Van Dolah, R. W.: The Chemistry of Nitrate Esters, *Chem. Rev.*, 55(3),
993 485–510, doi:10.1021/cr50003a001, 1955.
- 994 [Boyd, C. M., Sanchez, J., Xu, L., Eugene, A. J., Nah, T., Tuet, W. Y., Guzman, M. I. and Ng, N. L.: Secondary
995 organic aerosol formation from the \$\beta\$ -pinene+NO₃ system: effect of humidity and peroxy radical fate,
996 *Atmos. Chem. Phys.*, 15\(13\), 7497–7522, doi:10.5194/acp-15-7497-2015, 2015.](#)
- 997 Browne, E. C., Min, K.-E., Wooldridge, P. J., Apel, E., Blake, D. R., Brune, W. H., Cantrell, C. A., Cubison, M.
998 J., Diskin, G. S., Jimenez, J. L., Weinheimer, A. J., Wennberg, P. O., Wisthaler, A. and Cohen, R. C.:
999 Observations of total RONO₂ over the boreal forest: NO_x sinks and HNO₃ sources, *Atmos. Chem.*
1000 *Phys.*, 13(9), 4543–4562, doi:10.5194/acp-13-4543-2013, 2013.
- 1001 Carter, W., Cockeriii, D., Fitz, D., Malkina, I., Bumiller, K., Sauer, C., Pisano, J., Bufalino, C. and Song, C.: A
1002 new environmental chamber for evaluation of gas-phase chemical mechanisms and secondary
1003 aerosol formation, *Atmos. Environ.*, 39(40), 7768–7788, doi:10.1016/j.atmosenv.2005.08.040, 2005.
- 1004 [Chuang, W. K. and Donahue, N. M.: A two-dimensional volatility basis set – Part 3: Prognostic modeling
1005 and NO_x dependence, *Atmos. Chem. Phys. Discuss.*, 15\(12\), 17283–17316, doi:10.5194/acpd-15-
1006 17283-2015, 2015.](#)
- 1007 Darer, A. I., Cole-Filipiak, N. C., O'Connor, A. E. and Elrod, M. J.: Formation and stability of
1008 atmospherically relevant isoprene-derived organosulfates and organonitrates., *Environ. Sci. Technol.*,
1009 45(5), 1895–902, doi:10.1021/es103797z, 2011.
- 1010 Day, D. A., Liu, S., Russell, L. M. and Ziemann, P. J.: Organonitrate group concentrations in submicron
1011 particles with high nitrate and organic fractions in coastal southern California, *Atmos. Environ.*,
1012 44(16), 1970–1979, doi:10.1016/j.atmosenv.2010.02.045, 2010.
- 1013 Donahue, N. M., Robinson, A. L., Stanier, C. O. and Pandis, S. N.: Coupled partitioning, dilution, and
1014 chemical aging of semivolatile organics., *Environ. Sci. Technol.*, 40(8), 2635–43,
1015 doi:10.1021/es052297c, 2006.
- 1016 Fry, J. L., Rollins, A. W., Wooldridge, P. J., Brown, S. S., Fuchs, H. and Dub, W.: Organic nitrate and
1017 secondary organic aerosol yield from NO₃ oxidation of β -pinene evaluated using a gas-phase kinetics
1018 / aerosol partitioning model, *Atmos. Chem. Phys.*, 9(3), 1431–1449, 2009.
- 1019 Hilal, S., Karickhoff, S. and Carreira, L.: Prediction of the vapor pressure boiling point, heat of
1020 vaporization and diffusion coefficient of organic compounds, *QSAR Comb. Sci.*, 22(6), 565–574,
1021 doi:10.1002/qsar.200330812, 2003.

- 1022 Hildebrandt, L., Donahue, N. M. and Pandis, S. N.: High formation of secondary organic aerosol from the
1023 photo-oxidation of toluene, *Atmos. Chem. Phys.*, 9(9), 2973–2986, 2009.
- 1024 Hildebrandt Ruiz, L. and Yarwood, G.: Interactions between Organic Aerosol and NO_y: ~~Influence on~~
1025 ~~Oxidant Production~~, Austin, 5 TX. Prepared for the Texas AQRP (Project 12-012), by the University
1026 of Texas at Austin, and ENVIRON International Corporation, Novato, CA, available at:
1027 http://aqrp.ceer.utexas.edu/projectinfoFY12_13/12-012/12-012FinalReport.pdf, 2013.
- 1028 Hildebrandt Ruiz, L., Paciga, A., Cerully, K., Nenes, A., Donahue, N. M. and Pandis, S. N.: Aging of
1029 Secondary Organic Aerosol from Small Aromatic VOCs: Changes in Chemical Composition, Mass Yield,
1030 Volatility and Hygroscopicity, *Atmos. Chem. Phys. Discuss.*, 14, 31441–31481, 2014.
- 1031 Hu, K. S., Darer, A. I. and Elrod, M. J.: Thermodynamics and kinetics of the hydrolysis of atmospherically
1032 relevant organonitrates and organosulfates, *Atmos. Chem. Phys.*, 11(16), 8307–8320,
1033 doi:10.5194/acp-11-8307-2011, 2011.
- 1034 Jacobs, M. I., Burke, W. J. and Elrod, M. J.: Kinetics of the reactions of isoprene-derived hydroxynitrates:
1035 gas phase epoxide formation and solution phase hydrolysis, *Atmos. Chem. Phys.*, 14(17), 8933–8946,
1036 doi:10.5194/acp-14-8933-2014, 2014.
- 1037 Kebabian, P. L., Wood, E. C., Herndon, S. C. and Freedman, A.: A practical alternative to
1038 chemiluminescence-based detection of nitrogen dioxide: Cavity attenuated phase shift spectroscopy,
1039 *Environ. Sci. Technol.*, 42(16), 6040–6045, doi:10.1021/es703204j, 2008.
- 1040 Lindinger, W., Hansel, A., Jordan, A. and Hansel, A.: Proton-transfer-reaction mass spectrometry (PTR –
1041 MS): on-line monitoring of volatile organic compounds at pptv levels, *Chem. Soc. Rev.*, 27, 347–354,
1042 1998.
- 1043 Liu, S., Shilling, J. E., Song, C., Hiranuma, N., Zaveri, R. A. and Russell, L. M.: Hydrolysis of Organonitrate
1044 Functional Groups in Aerosol Particles, *Aerosol Sci. Technol.*, 46(12), 1359–1369,
1045 doi:10.1080/02786826.2012.716175, 2012.
- 1046 Matsunaga, A. and Ziemann, P. J.: Gas-Wall Partitioning of Organic Compounds in a Teflon Film Chamber
1047 and Potential Effects on Reaction Product and Aerosol Yield Measurements, *Aerosol Sci. Technol.*,
1048 44(10), 881–892, doi:10.1080/02786826.2010.501044, 2010.
- 1049 Ng, N. L., Chhabra, P. S., Chan, A. W. H., Surratt, J. D., Kroll, J. H., Kwan, A. J., McCabe, D. C., Wennberg,
1050 P. O., Sorooshian, A., Murphy, S. M., Dalleska, N. F., Flagan, R. C. and Seinfeld, J. H.: Effect of NO_x
1051 level on secondary organic aerosol (SOA) formation from the photooxidation of terpenes, *Atmos.*
1052 *Chem. Phys. Discuss.*, 7(4), 10131–10177, doi:10.5194/acpd-7-10131-2007, 2007.
- 1053 Ng, N. L., Herndon, S. C., Trimborn, A., Canagaratna, M. R., Croteau, P. L., Onasch, T. B., Sueper, D.,
1054 Worsnop, D. R., Zhang, Q., Sun, Y. L. and Jayne, J. T.: An Aerosol Chemical Speciation Monitor (ACSM)
1055 for Routine Monitoring of the Composition and Mass Concentrations of Ambient Aerosol, *Aerosol Sci.*
1056 *Technol.*, 45(7), 780–794, doi:10.1080/02786826.2011.560211, 2011.

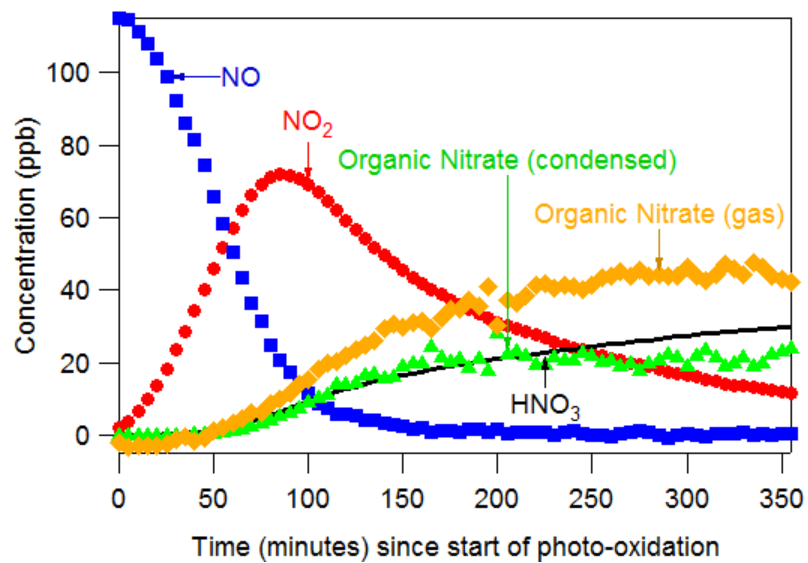
- 1057 Pankow, J. F.: An absorption model of gas/particle partitioning of organic compounds in the
1058 atmosphere, *Atmos. Environ.*, 28(2), 185–188, doi:10.1016/1352-2310(94)90093-0, 1994.
- 1059 Perraud, V., Bruns, E. a, Ezell, M. J., Johnson, S. N., Yu, Y., Alexander, M. L., Zelenyuk, A., Imre, D., Chang,
1060 W. L., Dabdub, D., Pankow, J. F. and Finlayson-Pitts, B. J.: Nonequilibrium atmospheric secondary
1061 organic aerosol formation and growth., *Proc. Natl. Acad. Sci. U. S. A.*, 109(8), 2836–41,
1062 doi:10.1073/pnas.1119909109, 2012.
- 1063 Perring, A. E., Bertram, T. H., Wooldridge, P. J., Fried, A., Heikes, B. G., Dibb, J., Crouse, J. D., Wennberg,
1064 P. O., Blake, N. J., Blake, D. R., Brune, W. H., Singh, H. B. and Cohen, R. C.: Airborne observations of
1065 total RONO₂: new constraints on the yield and lifetime of isoprene nitrates, *Atmos. Chem. Phys.*, 9(4),
1066 1451–1463, doi:10.5194/acp-9-1451-2009, 2009.
- 1067 Rindelaub, J. D., McAvey, K. M. and Shepson, P. B.: The photochemical production of organic nitrates
1068 from α -pinene and loss via acid-dependent particle phase hydrolysis, *Atmos. Environ.*, 100, 193–201,
1069 doi:10.1016/j.atmosenv.2014.11.010, 2015.
- 1070 Rollins, A. W., Pusede, S., Wooldridge, P., Min, K.-E., Gentner, D. R., Goldstein, A. H., Liu, S., Day, D. A.,
1071 Russell, L. M., Rubitschun, C. L., Surratt, J. D. and Cohen, R. C.: Gas/particle partitioning of total alkyl
1072 nitrates observed with TD-LIF in Bakersfield, *J. Geophys. Res. Atmos.*, 118(12), 6651–6662,
1073 doi:10.1002/jgrd.50522, 2013.
- 1074 Seinfeld, J. H. and Pandis, S. N.: *Atmospheric Chemistry and Physics*, 2nd ed., Wiley-Interscience, ~~72~~
1075 [Hoboken](#), 2006.
- 1076 [Wildt, J., Mentel, T. F., Kiendler-Scharr, A., Hoffmann, T., Andres, S., Ehn, M., Kleist, E., M \$\ddot{u}\$ sgen, P.,
1077 \[Rohrer, F., Rudich, Y., Springer, M., Tillmann, R. and Wahner, A.: Suppression of new particle
1078 \\[formation from monoterpene oxidation by NO_x, *Atmos. Chem. Phys.*, 14\\\(6\\\), 2789–2804,
1079 \\\[doi:10.5194/acp-14-2789-2014, 2014.\\\]\\\(#\\\)\\]\\(#\\)\]\(#\)](#)
- 1080 Winer, A. M., Peters, J. W., Smith, J. P. and Pitts, J. N.: Response of Commercial Chemiluminescent NO-
1081 NO, Analyzers to Other Nitrogen-Containing Compounds, *Environ. Sci. Technol.*, 8(13), 1118–1121,
1082 doi:10.1021/es60098a004, 1973.
- 1083
- 1084
- 1085
- 1086
- 1087
- 1088
- 1089

1090
 1091
 1092
 1093
 1094
 1095
 1096
 1097
 1098
 1099
 1100
 1101
 1102
 1103
 1104
 1105
 1106

Table 1. Experimental conditions and summary of results.

Exp	initial α -pinene (ppb)	initial NO (ppb)	RH (%)	H ₂ O ₂ conc in model (ppb) ^a	O ₃ (ppb) ^b	ON ^{aer} ($\mu\text{g}/\text{m}^3$) ^{b,c}	PM Org ($\mu\text{g}/\text{m}^3$) ^{b,c}	ON ^{gas} (ppb) ^b	Part coeff ^d	Hyd. (day ⁻¹)
1	40	30	22	100	90	7	90	13	0.19	NA ^e
2	40	40	39	60	50	6	60	11	0.18	2.2
3	40	40	0	40	50	4	30	13	0.10	NA ^e
4	130	110	68	600	210	150	1700			2.4
5	130	130	22	900	330	70	780	57	0.33	1.8
6	130	120	50	500	240	40	460	47	0.26	1.9
7	130	120	15	200	210	50	510	34	0.38	0.2
8	80	80	0	1000	300	30	310	32	0.26	0.6
9	80	80	0	1500	330	20	270	28	0.25	0.2
10	50	50	70	600	180	20	220			6.9
11	40	40	70	200	70	10	70			2.5
12	50	50	67	500	170	170	2200			5.2

^a H₂O₂ concentration for which SAPRC model most closely matched measurements of NO_x and O₃
^b Measured and averaged over a 20 minutes period when PM organics peaked
^c Corrected for wall-losses as described in Sect. 2.1.2
^d Molar basis
^e Experimental conditions resulted in aerosol growth throughout the experiment



1107

1108 Figure 1 – A time series of oxidized-nitrogen species in Expt. 77. NO, NO₂, and ON^{aer} are measured
 1109 directly. HNO₃ is modeled using SAPRC. ON^{gas} is calculated from a mass balance.

1110

1111

1112

1113

1114

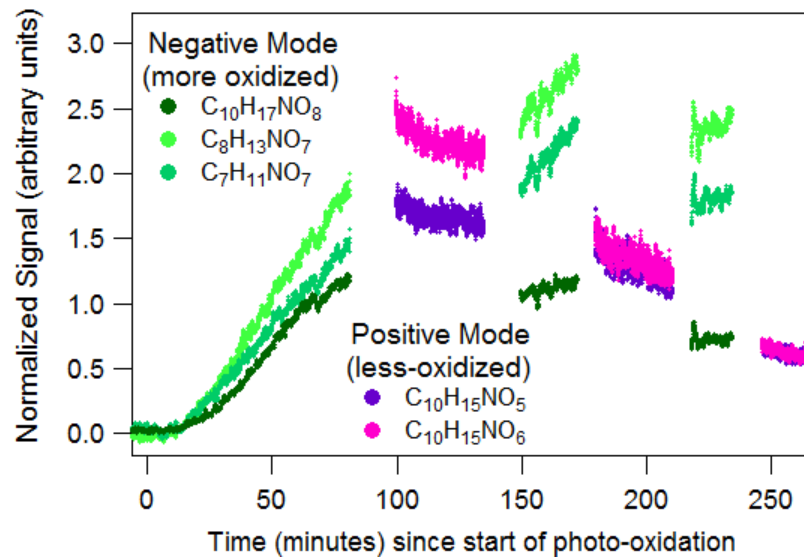
1115

1116

1117

1118

1119



1120

1121

Figure 2 – Time series of selected organic nitrates identified by HR-ToF-CIMS (Expt. 10)

1122

1123

1124

1125

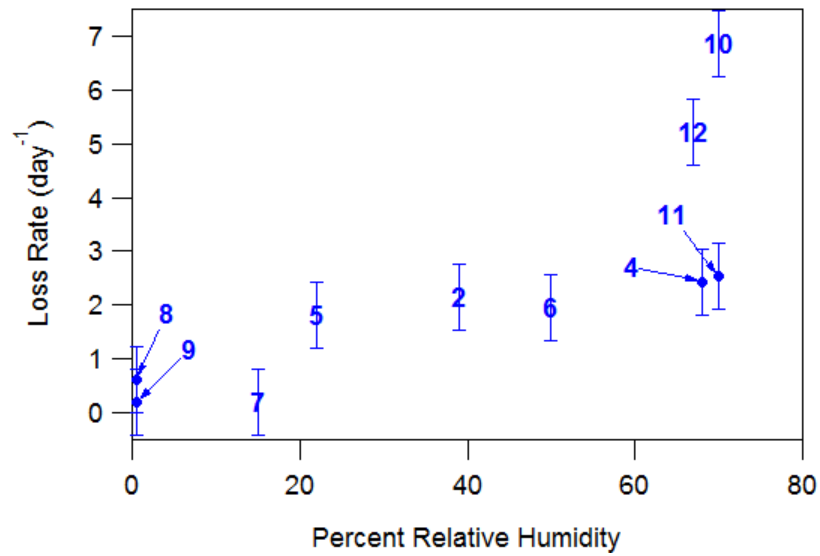
1126

1127

1128

1129

1130



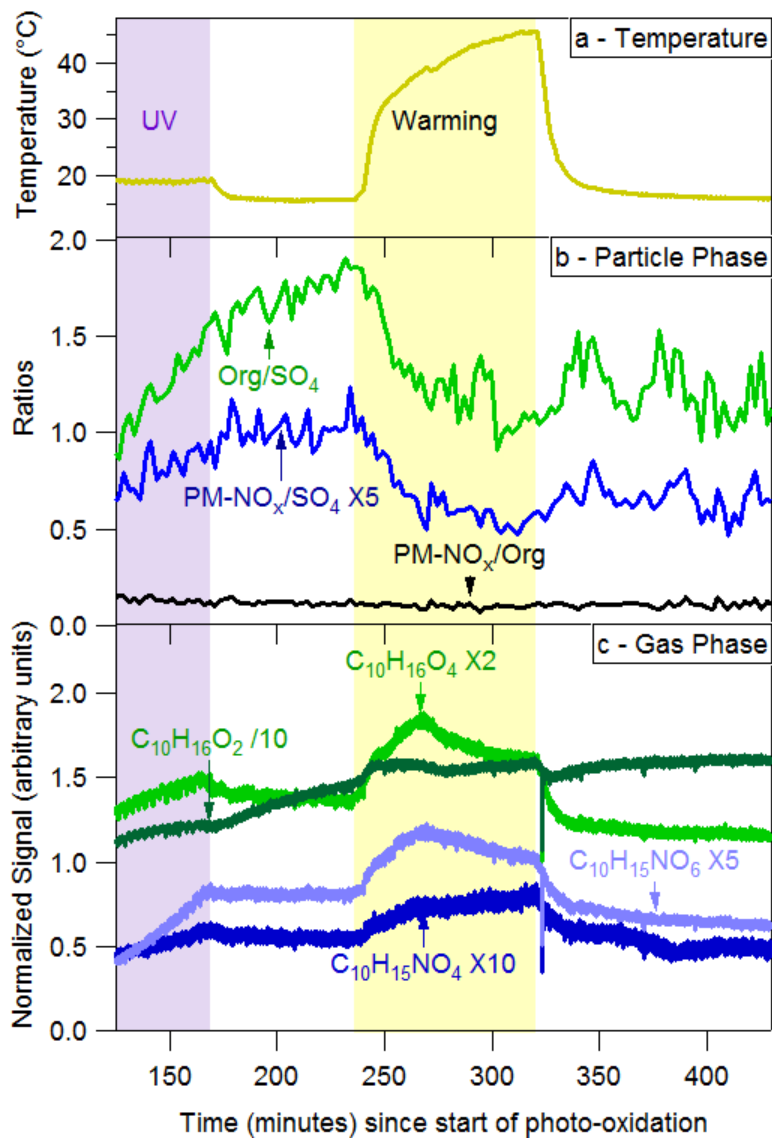
1131

1132

1133

1134

Figure 53. The organic nitrate loss rate as a function of relative humidity for Expts. 2-11, 4-12. Uncertainty (error bars) is estimated as 0.6 day⁻¹, the highest loss rate observed in experiments below 5% RH (Expt. 8).



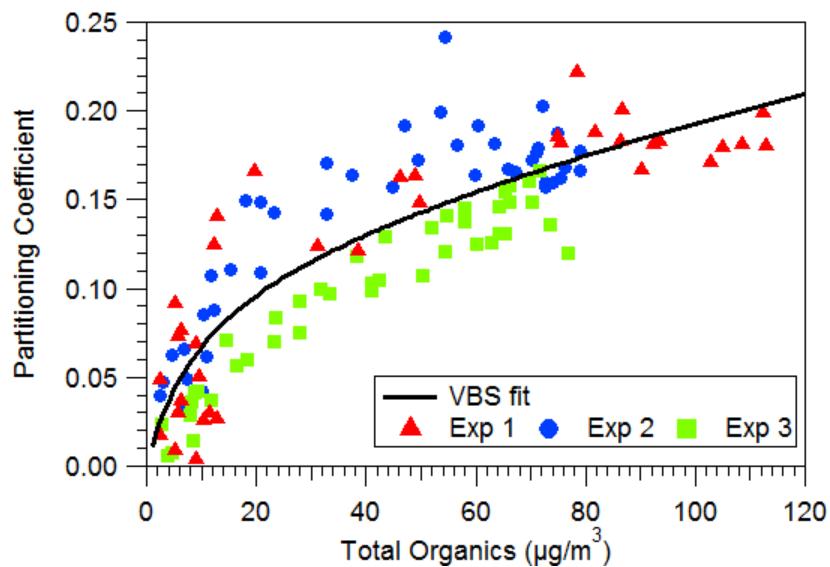
1135

1136

1137

1138

Figure 34 – Temperature effects on gas-particle partitioning of organic nitrates (Expt. 2).



1139

1140 Figure 45 – Volatility basis set fit from this work shown a) with data from Expts. 1, 2, and 3 and the VBS
 1141 fit from Rollins et al. (2013) and b) with data from Expts 1-3 and 5-9 (RH 0-50%).

1142

1143

1144

1145

1146

1147

1148

1149

1150